Supplemental material to this article can be found at:
http://molpharm.aspetjournals.org/content/suppl/2022/11/18/molpharm.122.000580.DC1
1521-0111/103/2/48–62$35.00
MOLECULAR PHARMACOLOGY
dx.doi.org/10.1124/molpharm.122.000580
Mol Pharmacol 103:48–62, February 2023

Multiplex G Protein–Coupled Receptor Screen Reveals Reliably Acting Agonists and a Gq-Phospholipase C Coupling Mode of GPR30/GPER1[S]

Nicole Urban, Marion Leonhardt, and Michael Schaefer

Medical Faculty, Rudolf-Boehm-Institute of Pharmacology and Toxicology, Leipzig University, Leipzig, Germany

Received June 17, 2022; accepted October 27, 2022

ABSTRACT

G protein–coupled receptors (GPCRs) constitute the most versatile family of pharmacological target proteins. For some "orphan" GPCRs, no ligand or drug-like modulator is known. In this study, we have established and applied a parallelized assay to coscreen 29 different human GPCRs. Three compounds, chlorhexidine, Lys-05, and 9-aminoacridine, triggered transient Ca^{2+} signals linked to the expression of GPR30. GPR30, also named G protein–coupled estrogen receptor 1 (GPER1), was reported to elicit increases in cAMP in response to 17β-estradiol, 4-hydroxytamoxifen, or G-1. These findings could, however, not be reproduced by other groups, and the deorphanization of GPR30 is, therefore, intensely disputed. The unbiased screen and following experiments in transiently or stably GPR30-overexpressing HEK293 cells did not show responses to 17β-estradiol, 4-hydroxytamoxifen, or G-1. A thorough analysis of the activated signaling cascade revealed a canonical G_q-coupled pathway, including phospholipase C, protein kinase C and ERK activation, receptor internalization, and sensitivity to the G_q inhibitor YM-254890. When expressed in different cell lines, the localization of a fluorescent GPR30 fusion protein appeared variable. An efficient integration into the plasma membrane and stronger functional responses were found in HEK293 and in MCF-7 cells, whereas GPR30 appeared mostly retained in endomembrane compartments in Cos-7 or HeLa cells. Thus, conflicting findings may result from the use of different cell lines. The newly identified agonists and the finding that GPR30 couples to G_q are expected to serve as a starting point for identifying physiologic responses that are controlled by this GPCR.

SIGNIFICANCE STATEMENT

This study has identified and thoroughly characterized novel and reliably acting agonists of the G protein–coupled receptor GPER1/GPR30. Applying these agonists, this study demonstrates that GPR30 couples to the canonical G_q-phospholipase C pathway and is rapidly internalized upon continuous exposure to the agonists.

Introduction

Representing one of the largest and most versatile groups of pharmacologically addressable target proteins, nonolfactory G protein–coupled receptors (GPCRs) are among the most intensively studied signaling proteins in mammals (Sriram and Insel, 2018). Thus, tremendous efforts have been undertaken to identify physiologic and pharmacological modulators of hitherto "orphan" GPCRs, with many substantial successes being reported within the last decades (Laschet et al., 2018; Hauser et al., 2020). Nonetheless, almost 100 orphan GPCRs are still awaiting the unequivocal assignment of cognate agonists and physiologic and pathophysiological functions governed by them. There are also "deorphanized" GPCRs whose assigned agonists or sites of expression are not reliably reproducible by other laboratories (Laschet et al., 2018), leading to partly confusing results pertaining to postulated receptor functions and proposed benefits of their modulation by pharmacological intervention. Finally, although not deorphanizing GPCRs by identifying a physiologic agonist, screening activities with or without prior virtual in silico prescreening have been instrumental in identifying drug-like compounds that exert agonistic effects or an inverse agonism toward individual orphan GPCRs.

We have established a Ca^{2+} influx-based academic screening infrastructure to identify cation channel-modulating activities in various compound libraries, comprising Food and Drug Administration–approved drugs, bioactive natural compounds, toxins, and chemically diverse drug-like compounds. To expand the range of investigated target structures, we conducted a first screening on GPR34, a GPCR whose deorphanization as a lysophosphatidyl-L-serine receptor (Sugo et al., 2006) has been questioned (Ritscher et al., 2012). Although screening results were valid, this screen failed to

This work was supported by the Deutsche Forschungsgemeinschaft (TRR-152, P18 to M.S.).
The authors declare no conflicts of interest.
dx.doi.org/10.1124/molpharm.122.000580.
[S] This article has supplemental material available at molpharm.aspetjournals.org.

ABBREVIATIONS: $[Ca^{2+}]_I$, intracellular Ca^{2+} concentration; CFP, cyan fluorescent protein; DAG, diacylglycerol; EPAC, exchange protein activated by cAMP; ER, endoplasmic reticulum; ERK, extracellular signal-regulated kinase; FRET, Förster resonance energy transfer; GPCR, G protein–coupled receptor; GPER1, G protein–coupled estrogen receptor 1; HBS, HEPES-buffered saline; InsP3, inositol-1, 4, 5-trisphosphate; PIP_2, phosphatidylinositol-4, 5 -bisphosphate; PKC, protein kinase C; PLC, phospholipase C; PTX, pertussis toxin; YFP, yellow fluorescent protein.

identify novel modulators. We therefore decided to explore the possibility to set up a highly parallelized coscreening that may become more successful in identifying novel agonists of orphan or poorly validated GPCRs in an unbiased fashion.

Typically, a high-throughput screening for GPCR agonists or antagonists requires the generation of a cell line that stably expresses a recombinant GPCR of interest, either alone or together with promiscuously coupling $G\alpha_{15/16}$ subunits or with chimeric G-protein α subunits that form a complex with endogenously expressed $\beta\gamma$ subunits. $G\alpha_{15/16}$ or chimeric $G\alpha_{q/i}$ subunits can be activated by GPCRs even if the receptor would otherwise couple to the G_s or $G_{i/o}$ families of heterotrimeric G proteins (Liu et al., 1995; Offermanns and Simon, 1995). At the effector side, $G\alpha_{15/16}$ or chimeric $G\alpha_{q/i}$ subunits activate phospholipases C (PLC), giving rise to formation of inositol-1,4,5-trisphosphate ($InsP_3$) and Ca^{2+} release via $InsP_3$ receptors that can be detected by means of fluorescent indicator dyes with exceptionally high signal-to-noise ratio (Kostenis et al., 2005). In preliminary cotransfection experiments, we added increasing numbers of GPCR-encoding plasmid constructs to transfection mixes that also contained expression plasmids that encode $G\alpha_{15}$ and $G\alpha_{16}$. Since functional signals were robustly detectable in a 384-well screening format with up to 15 coexpressed GPCR constructs, including G_i-coupling FP_1 formyl peptide and ET_B endothelin receptors, and the G_s-coupling V_{2A} vasopressin receptor, we embarked on a multiplex GPCR screen with two sets of expression plasmids that encode 15 or 14 GPCRs each. The sets were assembled based on the orphan character, a poorly identified function of the GPCR, or by a lack of drug-like modulators.

Among the coscreened receptors, GPR30 has been tentatively deorphanized as a plasma membrane- or endomembrane-resident estrogen receptor and, therefore, renamed by the International Union of Basic & Clinical Pharmacology as G protein–coupled estrogen receptor 1 (GPER1). Although initial reports provided evidence for G_s coupling, leading to cAMP formation (Filardo et al., 2002), or a noncanonical signaling pathway that includes phospholipase C-independent release of Ca^{2+} from internal storage organelles and formation of phosphatidylinositol-3,4,5-trisphosphate in the nucleus (Revankar et al., 2005), other studies found neither an activation by estrogens nor by other recently reported GPER1 agonists (Otto et al., 2008; Tutzauer et al., 2021). Due to the inconclusive data of agonist activities and downstream coupling, we included GPER1 in our unbiased screening and found no agonistic activity of estrogens or other reported GPER1 agonists. Instead, we identified three nonsteroidal drug–like compounds with agonistic properties toward GPR30. The signaling cascade was identified as a canonical G_q-/PLC-dependent pathway, leading to phosphatidylinositol-4,5-bisphosphate (PIP_2) hydrolysis, Ca^{2+} release from thapsigargin-sensitive stores, and protein kinase C activation. In addition, the newly identified GPR30 agonists efficiently trigger receptor clustering and internalization as a hallmark of effective agonism of the used ligands.

Materials and Methods

Chemicals. Chlorhexidine, Lys05, 9-aminoacridine, 17β-estradiol, 4-hydroxytamoxifen, fulvestrant, oleuropein, 3-hydroxytyrosol, niacin, niacin amide U-73122, and U-73433 were purchased from Sigma Aldrich (Munich, Germany). G-1 was ordered from Tocris (Wiesbaden-Nordenstadt, Germany), and YM-254890 was supplied by Biomol (Hamburg, Germany).

Molecular Biology Methods. Human estrogen receptor 1 (GPER1/GPR30) cloned into pcDNA3.1 was purchased from the cDNA Resource Center (Bloomsburg, PA). Subcloning into a custom-made mammalian expression vector that contains the open reading frame of yellow fluorescent protein (YFP) for C-terminal fusion to proteins of interest (pcDNA3-YFP; Schaefer et al., 2001) was carried out by polymerase chain reaction and primers (5′-gctcggatccactagtccagtgtg and 5′-gccctctagatgcacggcactg) to remove the stop codon, followed by digestion with Eco-RI/Xba-I. The gel-purified fragment was then ligated by T4 ligase into pcDNA3-YFP, and the absence of mutations was ascertained by sequencing the entire open reading frame.

Cell Culture and Transfections. HEK293 and HeLa cells were cultured in Earlés Minimum Essential Medium (Sigma, Munich, Germany), whereas COS-7 and MCF-7 cells were grown in Dulbecco's modified Eagle's medium and RPMI 1640 medium (Sigma, Munich, Germany), respectively. All media were supplemented with 10% fetal calf serum (Gibco Thermo Fisher Scientific, Darmstadt, Germany), 2 mM L-glutamine, 100 U/ml penicillin, and 0.1 mg/ml streptomycin.

For primary screening, HEK293 cells were seeded into 6-cm culture dishes and transfected with a mixture of 14 or 15 GPCRs, FP_1 formyl peptide receptor, YFP-tagged ET_B endothelin receptor, and $G\alpha_{15}$/$G\alpha_{16}$-encoding cDNA plasmids using the transfection reagent Lipofectamin 2000 (Invitrogen, Thermo Fisher Scientific). The total cDNA plasmid amount per transfection was 9.6 or 10.2 μg, and each single plasmid construct was added at an amount of 600 ng or 300 ng (GPR1, GPR4, GPR12, GPER1, $G\alpha_{15}$, $G\alpha_{16}$). A reduced cDNA amount was selected for the four GPCR isoforms because they suppressed signals of control receptors when transfected at higher amounts. For confocal laser-scanning microscopy and single-cell intracellular Ca^{2+} concentration ($[Ca^{2+}]_i$) imaging experiments, cells were plated onto 25-mm poly-L-lysine–coated glass coverslips. If required, these cells were transiently transfected with 2 μg of the respective pcDNA construct applying jetPEI Polyplus (PEQLAB, Erlangen, Germany) 24 hours after cell plating. To obtain a stably human GPR30-expressing HEK293 cell line ($HEK293_{hGPR30\text{-}YFP}$), cells were transiently transfected, and the growth medium was supplemented with 1 mg/ml geneticin. Stably transfected colonies were generated with a limiting dilution method and verified by fluorescence microscopy and functional assays. All cells were maintained at 37°C and in a 5% CO_2-aerated, humidified atmosphere.

Fluorometric $[Ca^{2+}]_i$ Imaging. All fluorometric Ca^{2+} assays were performed in HEPES-buffered saline (HBS), containing 132 mM NaCl, 6 mM KCl, 1 mM $MgCl_2$, 1 mM $CaCl_2$, 5.5 mM D-glucose, and 10 mM HEPES, adjusted to pH 7.4 with NaOH. For measurements in a Ca^{2+}-free buffer, we used a modified HBS in which $CaCl_2$ was omitted, and 200 μM EGTA were added before readjusting the pH.

For the primary screen, to generate concentration-response curves or in multiwell assays applying various GPCR signaling inhibitors, a custom-made fluorescence imaging plate reader built into a robotic liquid-handling station (Freedom Evo 150, Tecan, Männedorf, Switzerland) was used as previously described (Häfner et al., 2019). To this end, transiently or stably transfected HEK293 cells were detached with trypsin and loaded with 4 μM fluo-4/AM (Invitrogen) in HBS, containing 1% bovine serum albumin for 30 minutes at 37°C. Cells were washed by centrifugation, resuspended in HBS, and dispensed into pigmented, clear-bottom 384-well plates (Greiner, Frickenhausen, Germany). After mounting plates onto the fluorescence imaging plate reader, fluorescence signals were continuously recorded with a Zyla 5.5 camera (Andor, Belfast, UK) and under the control of Micromanager software (Edelstein et al., 2010). Fluo-4 was excited at 460–480 nm by using a projection of a light pipe–homogenized array of light-emitting diodes, and emission was detected through a 515-nM long-pass filter. After recording an initial baseline in each experiment, compounds of Selleckchem library or serially prediluted agonists or modulators were pipetted

with a 96-tip multichannel arm (MCA96, Tecan) in 4 quadrant steps (Q1 to Q4). Finally, fluorescence intensities were calculated from image stacks for each single well with ImageJ software, corrected for background signals and normalized to the initial intensities (F/F_0). Generation of concentration-response curves was done by fitting Hill equations (minimal effect E_{min}, maximal effect E_{max}, EC_{50}, and Hill coefficient n) to the data.

Single-cell $[Ca^{2+}]_i$ imaging analyses were performed on an inverted epifluorescence microscope (Carl Zeiss, Jena, Germany) and calibrated as described (Lenz et al., 2002). To this end, HEK293, COS-7, HeLa, or MCF-7 cells seeded onto 25-mm coverslips were loaded with 4 μM fura-2/AM (AAT Bioquest) for 30 minutes at 37°C in HBS, containing 0.2% bovine serum albumin f. Then, cells were rinsed, and coverslips were mounted in an HBS-filled bath chamber and sequentially excited at wavelengths of 340 nm, 358 nm, and 380 nm. Fluorescence emission was detected at 505–550 nm with a cooled charge-coupled device camera. After baseline recording, chlorhexidine, Lys05, 9-aminoacridine, or thapsigargin were added, and Ca^{2+} signals were monitored. Note, when 9-aminoacridine was applied, cells were loaded with 4 μM fluo-4/AM instead of fura-2/AM because this compound is fluorescent when excited at wavelengths that heavily overlap with those of the fura-2 excitation spectrum. Consequently, data are not expressed as $[Ca^{2+}]_i$ but as relative increases in fluorescence intensities.

Laser-Scanning Microscopy and Translocation Assays. The subcellular distribution of human GPR30 in various cell lines was visualized in living cells with an inverted confocal laser-scanning microscope (LSM510-META, Carl Zeiss, Oberkochen, Germany) using a 100x/1.46 alpha Plan-Apochromat objective and applying pinhole settings to yield optical slices with a thickness of 0.9–1.1 μM. Imaging of GPR30 internalization and cell blebbing during agonist stimulation was carried out by recording time series with 1 picture per minute.

Time-lapse analysis of cyan fluorescent protein (CFP)-PLCδ_1(PH) and protein kinase C ε (PKCε-CFP) translocation was also assessed with a 100x/1.46 alpha Plan-Apochromat objective but on an inverted epifluorescence microscope (Carl Zeiss, Jena, Germany) equipped with a monochromator (Polychrome V, TillVision, Gräfelfing, Germany) and a cooled charge-coupled device camera (IMAGO-QE, TillVision). $HEK293_{hGPR30\text{-}YFP}$ cells grown on coverslips were transfected with cDNA plasmids encoding CFP-tagged PLCδ_1(PH) or PKCε 24 hours prior to the experiments as previously described (Sinnecker and Schaefer, 2004). Coverslips were superfused with 5 μM chlorhexidine or Lys05, and translocation was recorded by CFP excitation at 410 nm and filtering the emission at 450–500 nm. To analyze the relative membrane association over the time, ratios of mean CFP fluorescence intensities over regions of interest defined over the plasma membrane and over the cytosol regions were calculated. Finally, data were normalized to the initial ratios measured before the application of GPR30 agonists.

Fluorometric Analysis of cAMP Formation. Monitoring of cAMP formation in $HEK293_{hGPR30\text{-}YFP}$ cells during GPR30 activation was performed using the fluorescence resonance energy transfer (FRET) sensor exchange protein activated by cAMP (EPAC) [mTurquoise2Δ-Epac(CD, ΔDEP)_td^{cp173}Venus, (Klarenbeek et al., 2015)]. All measurements were done in HBS on an inverted epifluorescence microscope (Carl Zeiss, Jena, Germany) equipped with a 25x/0.8 Plan-Neofluar objective 24 hours after transfecting cells with 2 μg of the EPAC biosensor-encoding cDNA plasmid. The sensor was sequentially imaged at three different spectral settings to obtain CFP-, YFP-, and FRET-prevalent settings: 1) excitation at 410 nm and emission at 450–500 nm, 2) excitation at 515 nm and emission at 530–600 nm, and 3) excitation at 410 nm and emission at 530–600 nm. Image triplets were obtained every second. After recording the baseline for 90 seconds, the respective GPCR agonist was added at the indicated final concentrations. After correction for background signals, mTurquoise and Venus fluorescence intensities and FRET efficiencies were calculated by multivariate linear regression analysis that compensates for channel crosstalk and differences in brightness of mTourquise, Venus, and mTourquise-Venus-FRET as described earlier (Lenz et al., 2002; Hellwig et al., 2004).

Imaging of Extracellular Signal-Regulated Kinase Activity with a FRET-Based Biosensor. Analysis of extracellular signal-regulated kinase (ERK) activation after GPR30 stimulation was executed using a cDNA plasmid encoding the cytosolic ERK activity reporter 4 (cytoEKAR4), which contains an ERK substrate peptide and reports its phosphorylation by an increase in the intramolecular FRET efficiency (Keyes et al., 2020). GPR30-expressing or parental HEK293 cells were transfected with 2 μg of the biosensor plasmid and measured after 24 hours on an inverted epifluorescence microscope (Carl Zeiss, Jena, Germany) equipped with a 25x/0.8 Plan-Neofluar objective. Fluorescence was excited at 410 nm, and images were sequentially obtained through emission bandpass filters at 450–490 nm and 530–600 nm mounted in a motorized filter wheel (Lambda 10-2, Sutter Instruments, Novato, CA). For analysis, emission ratios of background-corrected signals were calculated and finally normalized to initial signals. To determine statistical differences after the addition of chlorhexidine, Lys05, or EGF in comparison with basal FRET signals, photobleaching was corrected by fitting the data of unstimulated controls to a single exponential decay function.

Results

Identification of Novel GPR30 Agonists by a Multiplexed GPCR Screen. To identify novel agonists that act on orphan or poorly characterized GPCRs, we simultaneously transfected HEK293 cells with two groups of various GPCRs (Fig. 1A) and subjected them to a medium-throughput Ca^{2+} assay, applying 4770 compounds of the Selleckchem bioactive compound library. The two distinct transfection mixes served to further increase the number of screened target structures and also served as a counterscreen to omit compounds that exert off-target effects or stimulate receptors and ion channels expressed by the parental HEK293 cell line. Since some of the orphan GPCRs might not couple to G proteins that activate PLC and Ca^{2+} release from the endoplasmic reticulum (ER), we additionally cotransfected the cells with the murine G protein α subunit $G\alpha_{15}$ and its human counterpart $G\alpha_{16}$. As previously described, both $G\alpha_{15}$ and $G\alpha_{16}$ not only redirect receptor signaling of G_s- or G_i-coupled receptors to PLC activation and subsequent Ca^{2+} mobilization but also enhance PLC stimulation mediated by $G_{q/11}$- or $G\alpha_{14}$-coupled GPCRs (Offermanns and Simon, 1995). To control for the efficiency of $G\alpha_{15}/G\alpha_{16}$ -dependent conversion of signaling toward Ca^{2+} signals, we added the cDNA encoding the FP_1 formyl peptide receptor and the YFP-tagged ET_B endothelin receptor as positive controls into each transfection mix. The screening was valid when transfected HEK293 cells expressed the YFP-fused ET_B receptor, and each transfected and fluo-4/AM-loaded cell batch responded with a substantial Ca^{2+} signal upon the addition of 10 nM endothelin-1 and 100 nM fMLP (data not shown). During acute addition of compounds of the Selleckchem library at a final concentration of 20 μM to cells that were transfected with mixture 1 (Fig. 1, B–E), we recorded GPCR-characteristic immediate and transient fluorescence signals in wells that received chlorhexidine, Lys05, or 9-aminoacridine. This prompted us to identify the cDNA plasmids in transfection mixture 1 that confer the responsiveness to these compounds. After two rounds of generating cDNA mixes with lower complexity of added GPCR- and G protein–encoding plasmids, we revealed the single human GPER1-encoding plasmid to correlate with the responses to all three compounds independently of coexpressed $G\alpha_{15/16}$

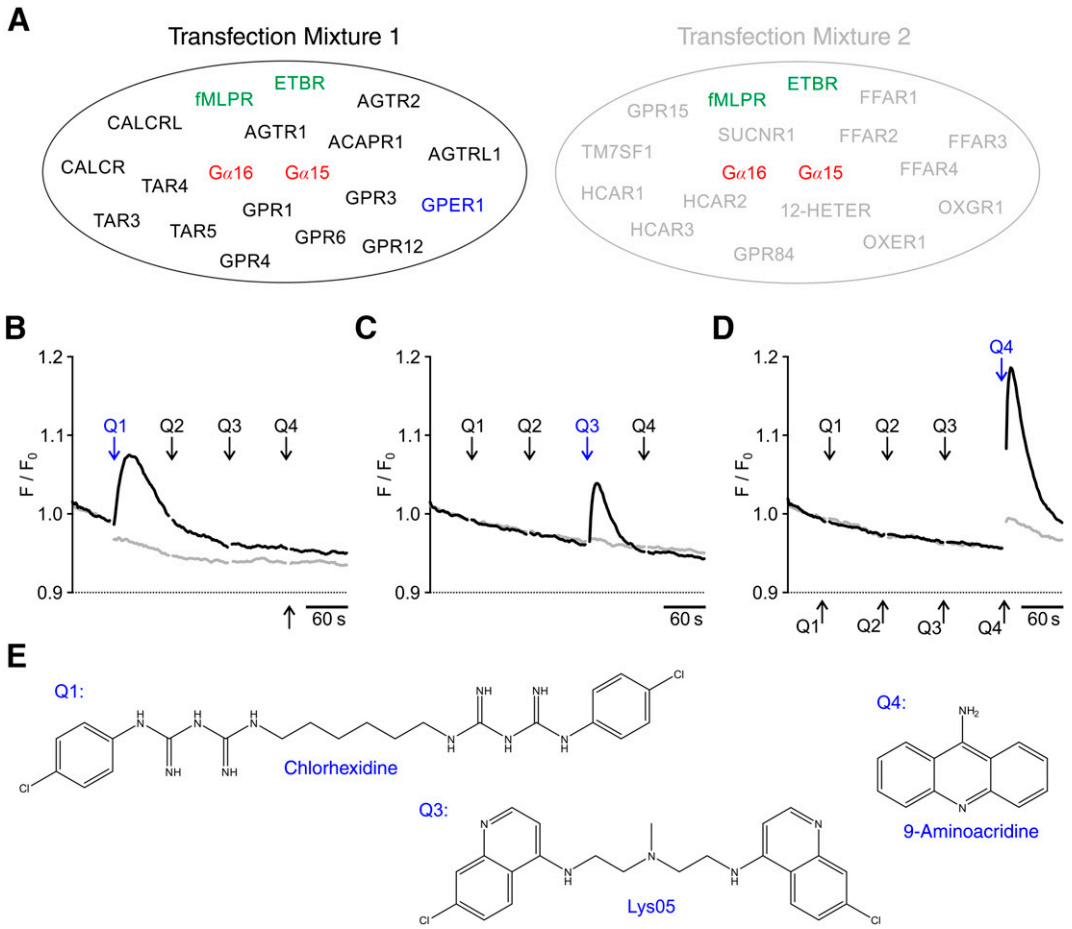

Fig. 1. Identification of new GPR30 agonists by a multiplexed GPCR screening. (A) HEK293 cells were transiently transfected with cDNA plasmid mixtures, encoding the indicated GPCRs, the FP_1 formyl peptide receptor, the C-terminally YFP-fused ET_B endothelin receptor, and the G-protein α_{15} and α_{16} subunits. Transfection mix 2 (right panel) contained cDNA plasmids, encoding 14 other GPCRs to be screened. (B–E) After 24 hours, both cell samples were subjected to a screen for novel GPCR agonists performing fluorometric Ca^{2+} assays in a 384-well microplate format. Cells were detached by trypsinization and loaded for 30 minutes with the Ca^{2+} indicator fluo-4/AM. After centrifugation and resuspension in HBS, cells were dispensed into black-pigmented, transparent-bottom 384-well plates. The multiwell plates were positioned on a fluorescence imaging plate reader built into a robotic liquid handling station. A 96-tip multichannel arm was used to inject and mix the 4718 compounds of a bioactive compound library (Selleckchem) at a final concentration of 20 μM, solvent controls or control agonists. Four pipetting steps in quadrants Q1–Q4 were required to apply compounds to all wells of the 384-well plates. To identify primary hits, wells showing a typical transient GPCR-induced rise in fluorescence intensity were compared between the two transfection mixtures. Chlorhexidine (B), Lys05 (C), and 9-aminoacridine (D) were the only compounds that elicited a robust $[Ca^{2+}]_i$ signal in cells transfected with mix 1 (black lines) but not after transfection with mix 2 (gray lines). (E) Chemical structures of the three screening hits.

(Supplemental Figs. 1 and 2). At a concentration of 10 μM, none of the three ligands caused a substantial Ca^{2+} mobilization in cells that expressed any of the other coscreened receptors in the presence or in the absence of coexpressed $G\alpha_{15}$ and $G\alpha_{16}$. Interestingly, published GPR30 agonists such as 17β-estradiol, 4-hydroxytamoxifen, fulvestrant, hydroxytyrosol, quercetin, oleuropein, niacin, or niacin amide, which were all included in the used compound library, did not elicit agonist-like properties during the primary screening.

Validation of Chlorhexidine, Lys05, and 9-Aminoacridine as GPR30 Agonists. For hit validation, we subcloned the purchased cDNA of human GPER1 into a custom-made pcDNA3-YFP vector to visualize the receptor expression and its cellular localization by monitoring the YFP fluorescence of the C-terminally tagged fusion protein. The generated plasmid construct (hGPR30-YFP) was used to generate a stably transfected HEK293 cell line ($HEK293_{hGPR30\text{-}YFP}$). The major subcellular localization of heterologously expressed hGPR30 seemed to be in the plasma membrane, with minor amounts of the YFP-tagged receptor protein residing in the endoplasmic reticulum as detected by confocal laser-scanning microscopy in living cells (Fig. 2A).

To assess the potency and efficacy of the newly identified GPR30 agonists, we loaded $HEK293_{hGPR30\text{-}YFP}$ with fluo-4/AM and measured the Ca^{2+} responses in our fluorescence imaging plate reader during the application of serially diluted agonist concentrations. Lys05 exerted the highest potency, with an EC_{50} of 270 nM, followed by the most efficient agonist chlorhexidine (EC_{50} = 750 nM). Since 9-aminoacridine is a strongly fluorescent dye, and to monitor for possible unspecific Ca^{2+} signals, we also applied the three compounds to the parental HEK293 cell line. We did not obtain any detectable rise in $[Ca^{2+}]_i$ when we incubated these cells with chlorhexidine, Lys05, or 9-aminoacridine within a concentration range of 0.02–40 μM (Fig. 2B). Next, we imaged GPR30 activation in adherent single GPR30-overexpressing HEK293 cells to estimate the levels of $[Ca^{2+}]_i$ reached by the addition of 5 μM chlorhexidine and Lys05, with the latter reaching

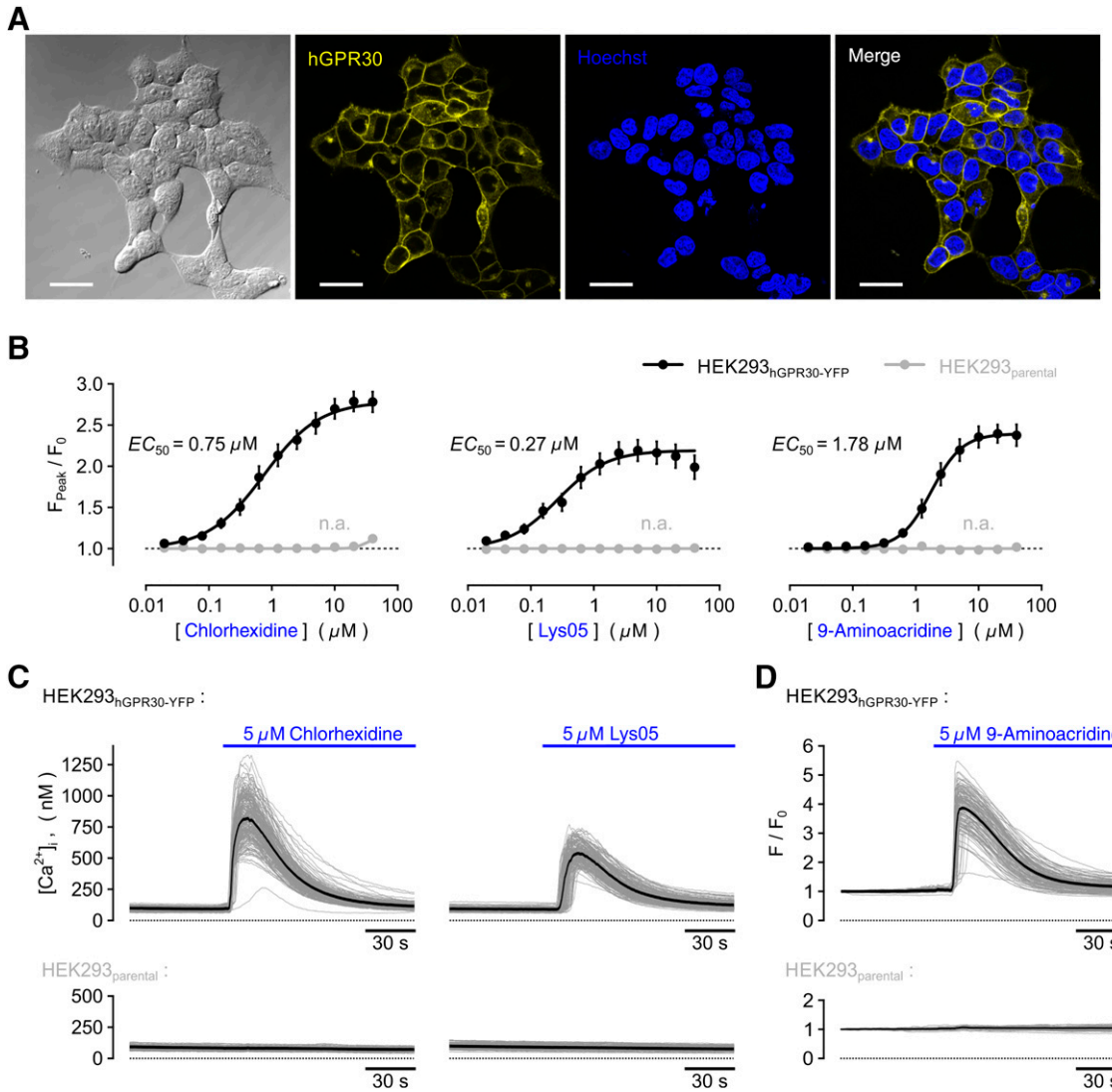

Fig. 2. $[Ca^{2+}]_i$ measurements in HEK293 cells stably expressing the human GPR30 during stimulation with new GPR30 agonists. (A) Confocal laser-scanning microscopy of living HEK293 cells stably overexpressing YFP-tagged human GPR30 ($HEK293_{hGPR30\text{-}YFP}$). Nuclei were counterstained with Hoechst 33258 and excited with a 405-nm laser. Scale bars, 30 μM. (B) Potency and efficacy of chlorhexidine, Lys05, and 9-aminoacridine were determined in multiwell Ca^{2+} assays using a fluorescence imaging plate reader device. Fluo-4–loaded $HEK293_{hGPR30\text{-}YFP}$ (black symbols and lines) or parental HEK293 (gray symbols and lines) cell suspensions were exposed to the serially diluted compounds, and Ca^{2+} signals were obtained as increases in fluorescence intensities compared with the respective basal intensities before agonist application (F/F_0). The indicated EC_{50} values were calculated by modeling the concentration-dependent peak Ca^{2+} responses (F_{Peak}/F_0) with a four-parameter Hill equation. Hill slopes were 0.98, 1.12, and 1.77 for chlorhexidine, Lys05, and 9-aminoacridine, respectively. Data represent means and S.E. of 6–10 independent biologic experiments performed in technical duplicates each. (C–D) Microfluorometric single-cell analysis of Ca^{2+} signals in $HEK293_{hGPR30\text{-}YFP}$ cells (upper panels) or in parental HEK293 cells (lower panels) during the application of chlorhexidine, Lys05, or 9-aminoacridine. Cells were loaded with fura-2/AM (C) or fluo-4/AM (D) and challenged with 5 μM of respective agonist. Shown is a representative measurement of 150–200 cells (gray lines) each. Averaged time courses for $[Ca^{2+}]_i$ or relative fluorescence intensities (F/F_0) are depicted as black lines.

somewhat lower maximal F/F_0 signals in multiwell assays. During stimulation, all cells responded with uniform and transient $[Ca^{2+}]_i$ signals that peaked after 5–15 seconds and almost decayed to baseline levels within 120 seconds, thereby excluding toxic effects on the cells. With regard to peak $[Ca^{2+}]_i$, the higher efficacy of chlorhexidine compared with Lys05 was confirmed by the calibrated single-cell $[Ca^{2+}]_i$ analysis. Single-cell Ca^{2+} imaging with 9-aminoacridine required the use of the indicator dye fluo-4 because the fluorescence excitation spectrum of 9-aminoacridine interferes with that of fura-2 (Fig. 2D). It should, therefore, be regarded as qualitative rather than quantitative data. When comparing concentration-response curves obtained in multiwell assays with fluo-4–loaded $HEK293_{hGPR30\text{-}YFP}$ cells, we found that F/F_0 values levels at saturating 9-aminoacridine concentrations ranged between those of chlorhexidine and Lys05. In parental HEK293 cells, 5 μM of the respective compounds failed to induce detectable increases in $[Ca^{2+}]_i$ in cell suspensions or in single-cell assays (Fig. 2, B–F). To test whether the identified agonists may act in an allosteric manner in relation to each other, we generated concentration-response curves with and without the addition of different submaximally effective concentrations of the respective other agonists. In case of a positive allosteric modulation, we would expect a shift of half-maximally effective concentrations to lower values. In none of the tested combinations did we observe such signs of allosteric modulation (Supplemental Fig. 3). As shown in Fig. 2B, high concentrations of Lys05 caused a

partial inhibition of $[Ca^{2+}]_i$ signals, which was also evident when applied in combination with chlorhexidine (Supplemental Fig. 3, A and C).

Since none of the previously reported GPR30 agonists appeared active in the primary multiplexed GPCR screening, we selected some relevant and most frequently used GPR30-activating drugs (Rosano et al., 2016) and generated concentration-response curves using our stably transfected $HEK293_{hGPR30\text{-}YFP}$ cell line as well as parental HEK293 cells. Surprisingly, only 4-hydroxytamoxifen and niacin amide led to an increase in fluorescence intensities when added at concentrations higher than 10 μM (Supplemental Fig. 4). Since they did so in $HEK293_{hGPR30\text{-}YFP}$ cells, and also in untransfected parental HEK293 cells, we consider them as presumably hGPR30-unrelated background signals. Other reported GPR30 agonists, including 17β-estradiol and G-1, which have been described to mobilize Ca^{2+} in MCF-7 and SKBr3 cells (Ariazi et al., 2010), were inactive in $HEK293_{hGPR30\text{-}YFP}$ cells as well as in parental HEK293 cells over the entire range of applied concentrations (Supplemental Fig. 4, A and B). If previously reported GPR30 agonists were biased to induce a G_i-coupling mode of the receptor, $[Ca^{2+}]_i$ assays might require a G_q priming (Pfeil et al., 2020) or coexpression with the promiscously coupling G proteins to detect a receptor activation by these agonists. However, neither G_q priming via stimulation of an endogenous muscarinic receptor with 100 μM carbachol nor coexpression of $G\alpha_{15}$ and $G\alpha_{16}$ led to Ca^{2+} signals upon challenging GPR30-expressing HEK293 cells with 17β-estradiol, G-1, or several other reported GPR30 agonists (Supplemental Fig. 4). Notably, the same G_q priming procedure or coexpression of $G\alpha_{15}$ and $G\alpha_{16}$ enhanced Ca^{2+} signals elicited via a G_i-coupled fMLP receptor.

Inhibition of GPR30-Triggered Ca^{2+} Signals by Gq, PLC, and $InsP_3$ Receptor Inhibitors. Signaling of G_q/G_i-coupling GPRCs typically triggers a Ca^{2+} release from $InsP_3$-sensitive Ca^{2+} stores. To strengthen the assumption that chlorhexidine, Lys05, and 9-aminoacridine mediate Ca^{2+} release from $InsP_3$-sensitive stores, we repeated microfluorometric single-cell $[Ca^{2+}]_i$ analyses using a Ca^{2+}-free bath solution. As expected, the Ca^{2+} mobilization response remained detectable under this condition, with response amplitudes of about two- to 2.5-fold compared with the respective basal levels (Fig. 3). Moreover, we depleted these stores by preincubating cells for 5 minutes with 2 μM thapsigargin, an inhibitor of endoplasmic reticulum Ca^{2+}-ATPases. In thapsigargin-treated $HEK293_{hGPR30\text{-}YFP}$ cells, chlorhexidine, Lys05, or 9-aminoacridine failed to elicit $[Ca^{2+}]_i$ signals, indicating that their signaling critically relies on the canonical PLC- and $InsP_3$-dependent Ca^{2+} mobilization pathway. To characterize GPR30 signaling in more detail, we incubated $HEK293_{hGPR30\text{-}YFP}$ cells either with the G_q inhibitor YM-254890 (1 μM), the phospholipase C inhibitor U-73122 (10 μM) or its inactive anolog U-73343 (10 μM), and with the $InsP_3$ receptor inhibitor 2-APB (100 μM) for 5 minutes. Then, GPR30 was challenged with the three new identified agonists. In contrast to solvent-treated control cells, Ca^{2+} rises were prevented when applying the inhibitors. U-73343 showed a very slight reduction of the maximal control signal during activation by Lys05 or 9-aminoacridine (Fig. 4). Since GPR30-dependent $[Ca^{2+}]_i$ signals were fully abrogated by the G_q inhibitor YM-254890, we assume that GPR30 activates phospholipase C, and Ca^{2+} mobilization at least in part via a G_q-coupling component. Since a combined G_q/G_i-coupling mode may be sensitive to YM-254890 as well (Pfeil et al., 2020), we used a pretreatment with pertussis toxin (PTX), which uncouples GPCRs from $G\alpha_{i/o}$ proteins and, thus, disrupts receptor signaling via G_i. To this end, we transiently cotransfected HEK293 cells with GPR30 and the FP_1 and ET_B receptors as positive controls for exclusively (FP_1) or predominantly (ET_B) G_i-coupling receptors. The G_q-coupled muscarinic M_3 acetylcholine receptor that is endogenously expressed in our HEK293 cell line served as a control for a PTX-resistant pathway. After treatment of cells with 100 ng/ml PTX or its solvent for 18–20 hours added to the culture medium, responses elicited by the GPCR agonists were analyzed in multiwell Ca^{2+} measurements. PTX-treated cells did not respond to 100 nM fMLP, and endothelin-1 (10 nM) signals were diminished by about 50% compared with untreated controls, thereby confirming the coupling behavior of pure G_i or mixed G_q/G_i coupling known for formyl peptide and endothelin receptor type B receptors. Activation of GPR30, applying either 5 μM chlorhexidine, Lys05, or 9-aminoacridine, as well as M_3 receptor activation by 100 μM carbachol were unaffected by pretreatment with PTX (Fig. 5). We therefore conclude that hGPR30 genuinely couples to the G_q-signaling cascade when challenged with the newly identified agonists.

Activation of GPR30 Results in Phosphoinositide Hydrolysis and Diacylglycerol Formation. In general, agonist binding to a G_q-coupling receptor results in an immediate activation of phospholipases C that hydrolyze PIP_2 to $InsP_3$ and diacylgylcerol (DAG). Since Revankar et al. (2005) described an inefficacy of PLC inhibitor U73122 on blocking GPR30-initiated calcium mobilization and thereby suggested a divergent signaling pathway, we extended the analysis of hGPR30 coupling to PLC, applying more direct methods. PIP_2 hydrolysis and DAG formation can be monitored by subcellular translocation of well characterized biosensor proteins. The plasma membrane PIP_2 content is reflected by the association of a CFP-fused pleckstrin homology domain of PLC-δ_1 [CFP-PLC-δ_1(PH)] to the plasma membrane. Upon PLC-mediated PIP_2 hydrolysis, CFP-PLC-δ_1(PH) translocates to the cytosol. Conversely, a translocation of CFP-tagged, DAG-sensitive novel protein kinase C ε isoform (PKCε-CFP) from the cytosol to the plasma membrane indicated DAG formation by PLC.

We transfected a CFP-PLC-δ_1(PH)–encoding plasmid into $HEK293_{hGPR30\text{-}YFP}$ cells and imaged the CFP-PLC-δ_1(PH) distribution during the addition of chlorhexidine or Lys05 by confocal microscopy and by epifluorescence time-lapse microscopy (Fig. 6, A–F). Within a few seconds after agonist application, the plasma membrane association of CFP-PLC-δ_1(PH) was markedly reduced and partly recovered within the following 5 minutes. Measurements of DAG formation were also performed by a translocation assay. Accordingly, we tracked transiently transfected PKCε-CFP, which was recruited from the cytosol to the plasma membrane upon the application of chlorhexidine or Lys05 (Fig. 6, G–L). Finally, we transiently expressed CFP-PLC-δ_1(PH) and PKCε-CFP in parental HEK293 and repeated the experiments. None of the proteins or agonists exerted detectable changes in the distribution of the biosensor proteins in the absence of GPR30 expression, whereas stimulation of a cotransfected histamine H_1 receptor served as a positive control (Supplemental Fig. 5).

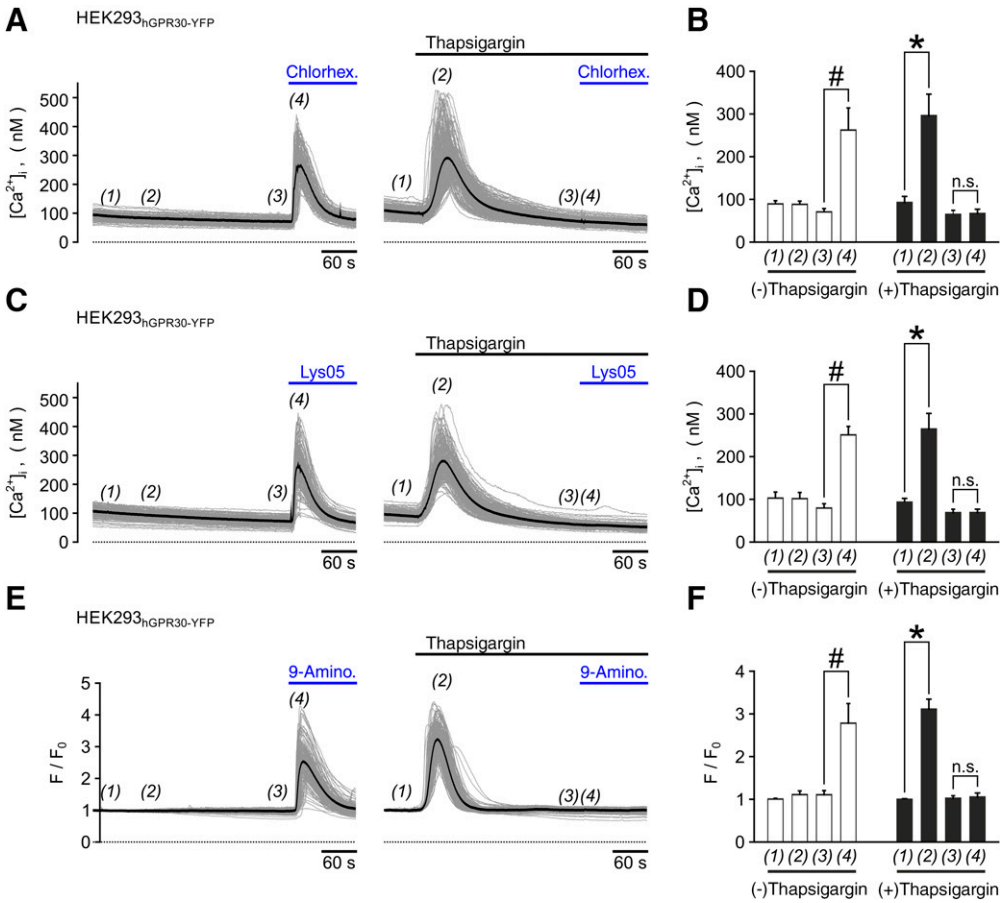

Fig. 3. Single-cell analysis of hGPR30-induced $[Ca^{2+}]_i$ signals in the absence of extracellular Ca^{2+} and after depletion of thapsigargin-sensitive intracellular Ca^{2+} stores. Microfluorometric analysis of $[Ca^{2+}]_i$ in $HEK293_{hGPR30\text{-}YFP}$ cells as described in Fig. 2C but in a nominally Ca^{2+}-free bath solution. (A, C, and E) Representative experiments depicting the application of 5 μM chlorhexidine, Lys05, or 9-aminoacridine to $HEK293_{hGPR30\text{-}YFP}$ cells without (left panels) and with prior incubation with 2 μM thapsigargin (right panels). Gray lines depict responses in single cells; black lines depict the average signal of all cells measured in this single biologic experiment. (B, D, and F) Statistical analysis of $[Ca^{2+}]_i$ signals (means and S.D.) obtained in four to five independent biologic experiments, performed as shown in (A, C, and E), each. Bars represent the time points as indicated in (A, C, and E). Increases in $[Ca^{2+}]_i$ after agonist stimulation (timepoints 4 versus 3) were seen in Ca^{2+}-free buffer (white bars) but not when applied after store depletion with thapsigargin (black bars). # or *, $P < 0.05$, Student's t test with paired data. n.s., no statistically significant difference.

Cyclic Adenosine Monophosphate Does Not Rise after Stimulation with GPR30 Agonists. The discovery of GPR30 as a putative membrane-resident estrogen receptor started with the observation that estrogen could activate adenylyl cyclase activity in MCF-7 cells, giving rise to the production of cAMP (Aronica et al., 1994). Later on, the GPR30 cDNA was cloned out of this cell line (Carmeci et al., 1997). Finally, Thomas et al. (2005) identified GPR30 as a G protein–coupled membrane receptor that is directly activated by estradiol and triggered increases in cytosolic cAMP concentrations. The cAMP generation mediated by GPR30 could, likewise, be confirmed by applying other agonists like G-1 or tamoxifen (Mo et al., 2013). Hence, we determined the cAMP formation in $HEK293_{hGPR30\text{-}YFP}$ cells during stimulation with chlorhexidine or Lys05. We applied the well established EPAC-derived cAMP biosensor to sensitively monitor cAMP formation in living cells in a time-resolved manner (Klarenbeek et al., 2015). Since elevation of cAMP would cause a decline in FRET efficiencies, we first validated the EPAC sensor by utilizing β-adrenergic and adenosine receptor agonists that act on Gs-coupled receptors that are endogenously expressed in HEK293 cells. The addition of epinephrine or adenosine rapidly and robustly reduced the initial FRET efficiency of 63%-64% to about 36%-18%, whereas solvent controls led only to a decrease in FRET efficiency, caused by photobleaching of the FRET acceptor (Fig. 7, B and C). FRET signals upon the addition of 5 μM 17β-estradiol or G-1 did not display discernible differences to those observed after the addition of HBS buffer. Likewise, the addition of chlorhexidine and Lys05 gave rise to FRET signals that were not different from those in solvent-treated controls (Fig. 7, A and C). To assess whether a coupling to the cAMP cascade may be restricted to certain cell types, we repeated assays in MCF7 cells that have been reported to express GPR30 (Carmeci et al., 1997). Neither 17β-estradiol nor G-1 induced a cAMP response as indicated by a coexpressed EPAC-derived cAMP biosensor (Supplemental Fig. 6). We thus exclude a predominant coupling of hGPR30 to the G_s-/adenylyl cyclase/cAMP pathway when challenged with previously reported or newly identified GPR30 agonists.

ERK Activation Assay. Coupling to the Ras-Raf-MEK-ERK pathway is a typical hallmark of G_q-coupled receptors. To assess the activity of this cascade in HEK293 cells, we coexpressed GPR30 with a cytosolic FRET-based ERK biosensor protein (cytoEKAR4) that reports the phosphorylation state of an ERK substrate by an increase in the intramolecular FRET efficiency (Keyes et al., 2020). As shown in Fig. 8, A–D, 5 μM chlorhexidine or 5 μM Lys05 caused an increase in FRET signals, with a maximum appearing about 10 minutes after agonist application and reaching an amplitude of about 40%–60% of maximal responses that were exerted by 100 ng/ml recombinant epidermal growth factor. Responses to chlorhexidine or Lys05 were absent in HEK293 cells that expressed the reporter protein but no GPR30 (Fig. 8, E–H).

Rapid Internalization of GPR30 and Potential Coupling to $G\alpha_{12/13}$. A characteristic feature of efficient and sustained GPCR activation is given by the receptor internalization, which uncouples the GPCR from G-protein signaling and may

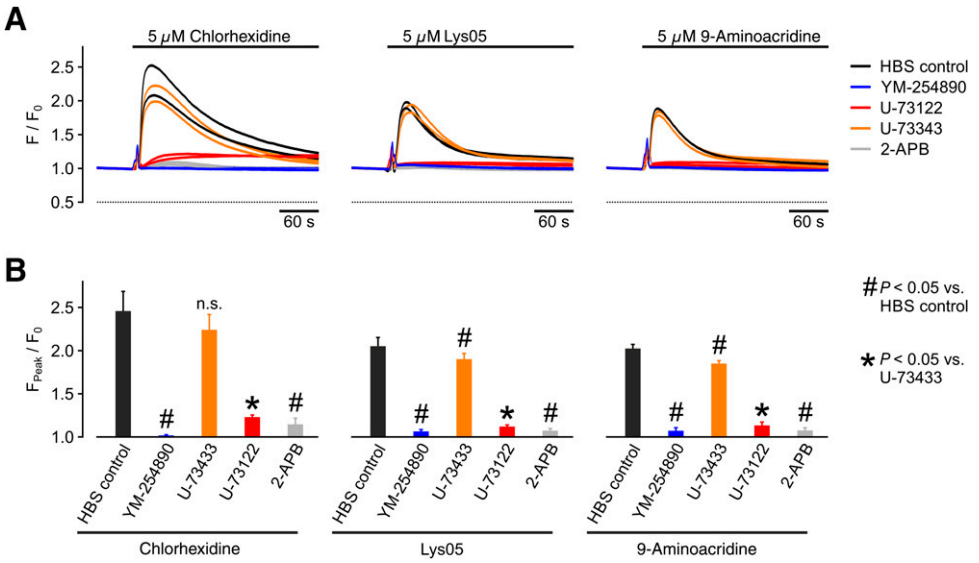

Fig. 4. GPR30-induced Ca^{2+} release is suppressed by Gq, PLC, and $InsP_3$ receptor inhibitors. (A) Representative fluorescence imaging plate reader analyses of fluo-4–loaded $HEK293_{hGPR30\text{-}YFP}$ cell suspensions after 5 minutes of preincubation without (HBS control) and with 1 μM YM-254890 (Gq inhibitor), 100 μM 2-APB (IP_3 receptor inhibitor), 10 μM U-73122 (PLC inhibitor), or U-73343 (inactive U-73122 analog). GPR30 was activated either by chlorhexidine (left panel), Lys05 (middle panel), or 9-aminoacridine (right panel). Shown are the kinetics of relative fluorescence intensities during stimulation, each condition as duplicate. Pipetting artifacts caused during compound application are not deleted. (B) Aggregated data (means and S.D.; n = 3 independent biologic experiments performed in technical duplicates each) of peak fluorescence intensities (F_{Peak}/F_0) measured as shown in (A). All blockers acting on G_q-mediated Ca^{2+} release were effective (# or *, $P < 0.05$ by one-way ANOVA with Dunn-Šidák post hoc test). Note that U-73343 only suppressed a minor fraction of Lys05- and 9-aminoacridine–induced responses, and effects on chlorhexidine-stimulated cells were statistically not significant (n.s.).

be followed either by terminal degradation in lysosomes or by receptor recycling back to the plasma membrane. To follow these processes, we imaged the subcellular localization of the YFP-fused hGPR30 during prolonged agonist application by using confocal laser-scanning microscopy. Upon the addition of 5 μM chlorhexidine or Lys05 that cause comparable amplitudes of Ca^{2+} responses, a clustered ("patchy") distribution and first distinct internalization patterns were already observable 2 minutes

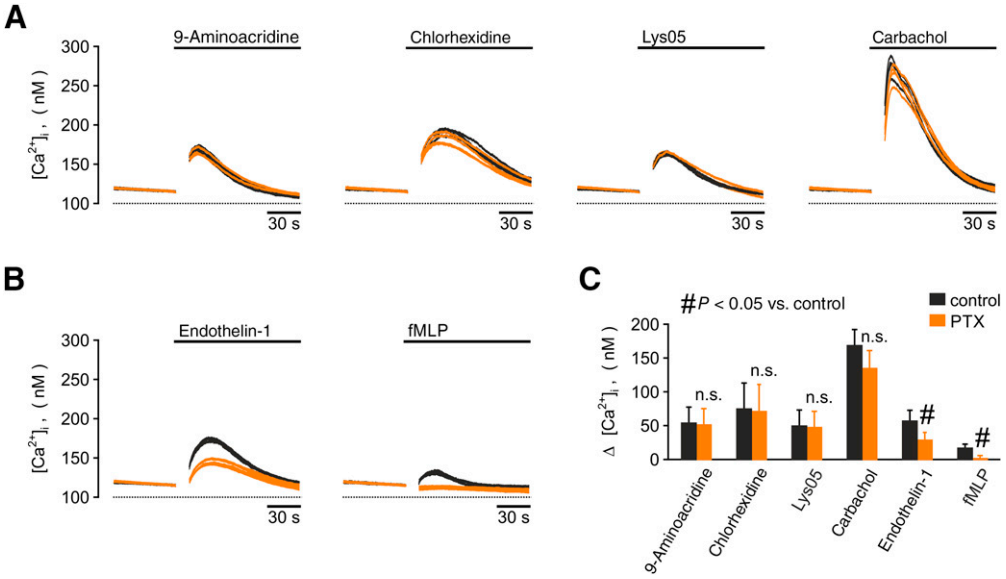

Fig. 5. Effect of PTX on GPR30-induced $[Ca^{2+}]_i$ signals. Similar fluorescence imaging plate reader experiments as in Fig. 4 but with HEK293 cells that transiently expressed human GPR30, the ET_B receptor, and the FP_1 formyl peptide receptor. Six hours after transfection, PTX (100 ng/ml) was added to the culture medium and incubated overnight to deactivate $G\alpha_{i/o}$ proteins by ADP ribosylation. The next day, cells were loaded with fluo-4 and subjected to multiwell Ca^{2+} imaging. (A and B) Shown are time courses of $[Ca^{2+}]_i$ obtained in a representative experiment during the addition of 5 μM 9-aminoacridine, 5 μM chlorhexidine, 5 μM Lys05, or the control agonists 100 μM carbachol, 10 nM endothelin-1, and 100 nM fMLP. Orange lines: data from four wells containing PTX-treated cells; black lines: four wells with untreated control cells from same transfection day. To exclude confounding effects of different cell numbers in single wells, the $[Ca^{2+}]_i$ was calibrated in each well at the end of the experiment. To this end, 0.04% Triton X-100 and 10 mM EGTA were sequentially added to expose the indicator to high (1 mM) and to very low (<20 nM) Ca^{2+} concentrations, respectively. (C) Statistical analysis of PTX-treated (black bars) and -untreated cells (white bars). Shown are means and S.D. (n = 4 independent biologic experiments, each performed in duplicates) of maximal $[Ca^{2+}]_i$ increases ($\Delta[Ca^{2+}]_i$) after adding the indicated agonists. Differences (#$P < 0.05$, Dunn–Šidák post hoc test) were only registered during activation of G_i-coupling ET_B or FP_1 receptors but not after stimulating endogenous muscarinic acetylcholine receptors or after applying hGPR30 agonists. n.s., statistically not significant.

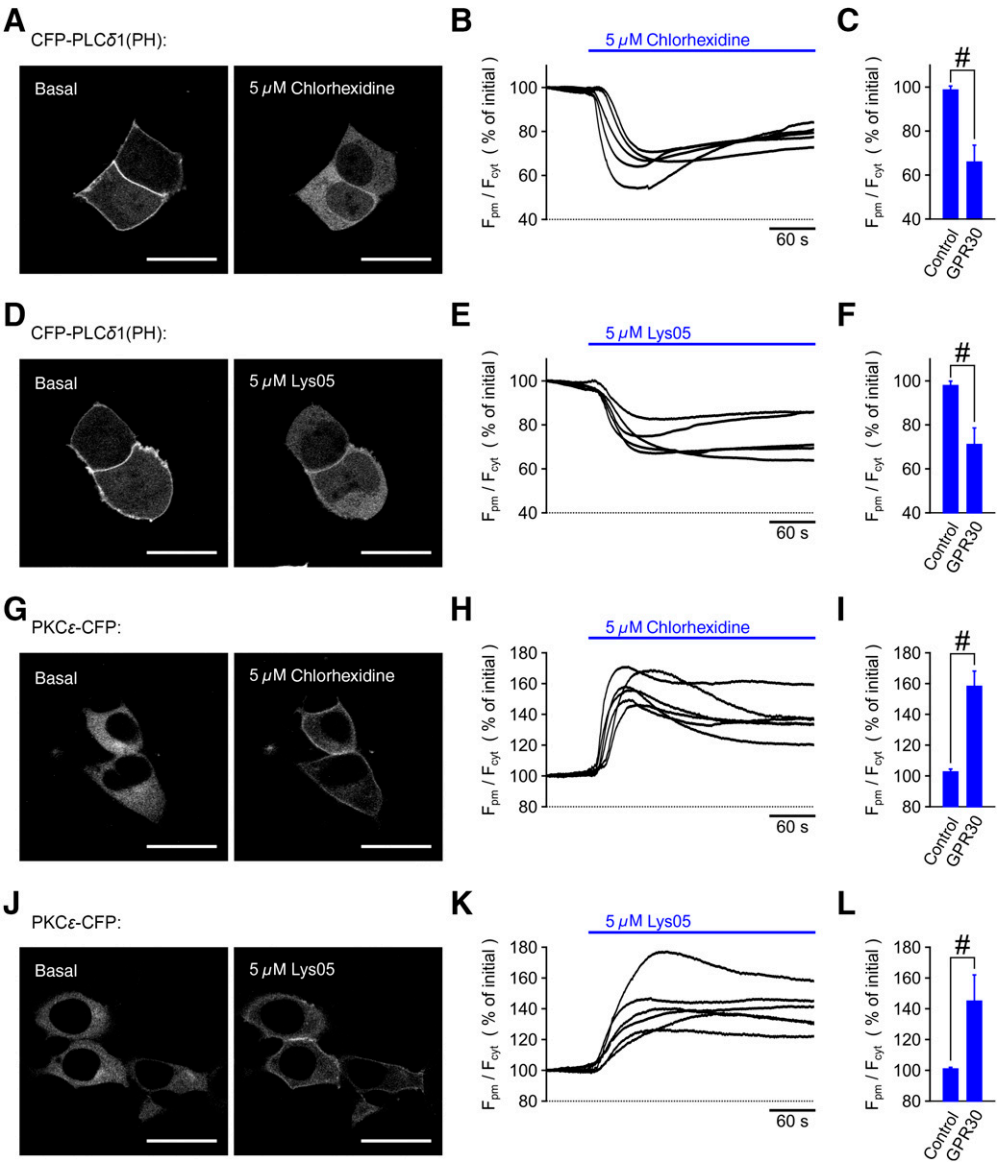

Fig. 6. Imaging of CFP-PLC-δ_1(PH) and PKCε-CFP translocation in HEK293$_{\text{hGPR30-YFP}}$ cells induced by chlorhexidine and Lys05 addition. HEK293$_{\text{hGPR30-YFP}}$ cells were transiently transfected with cDNA plasmids encoding the pleckstrin homology domain of phospholipase C-δ1 N-terminally fused to CFP [CFP-PLC-δ_1(PH); A–F] or a protein kinase C ε C-terminally fused to CFP (PKCε-CFP; G–L). (A, D, G, and J) Confocal microscopy images of the CFP-fused translocating biosensor proteins in unstimulated (left panels) and in chlorhexidine- or Lys05-stimulated cells (right panels). Scale bars, 20 μM. (B, E, H, and K) Typical time courses of relative changes of PLC-δ_1(PH) or PKCε fluorescence signals measured by time-lapse epifluorescence microscopy in regions of interest defined over the plasma membrane (F_{pm}) and the cytosol (F_{cyt}) of the same cells, expressed as ratios and normalized to the initial values. Shown are data from five to six independent experiments, each comprising four to nine measured cells. (C, F, I, and L) Statistical comparison (#$P < 0.05$, Student's t test with unpaired data) of strongest PLC-δ_1(PH) or PKCε-CFP translocation effects seen in GPR30-expressing (GPR30) or in parental HEK293 (control) cells after the addition of chlorhexidine (C and I) or Lys05 (F and L) observed in n = 5 to 6 independent experiments each.

after agonist application (Fig. 9, A and B). Within 10–20 minute, hGPR30-YFP was almost quantitatively removed from the plasma membrane in chlorhexidine- or Lys05-treated cells. 9-Aminoacridine seemed to be slower acting, but within 20 minutes, GPR30 followed the same clustered distribution and substantial internalization as seen with the other two agonists (Fig. 9C). In the transmitted light channel, a secondary finding while imaging chlorhexidine- or Lys05-stimulated HEK293 cells overexpressing hGPR30 was a marked membrane blebbing. To visualize the blebbing events independently of hGPR30 clustering and internalization, we stably transfected HEK293$_{\text{hGPR30-YFP}}$ cells with an expression plasmid that encodes a CAAX-box–modified and thereby membrane-targeted CFP. During hGPR30 internalization mediated by chlorhexidine or Lys05, the CFP-CAAX protein indicated distinct bleb-like bulges in the plasma membrane (Fig. 10) that may reflect a rearrangement of the cortical actin network (Charras, 2008). Since GPCR coupling to G$\alpha_{12/13}$ is known to affect the actin cytoskeleton through the downstream effectors RhoA and ROCK (Purvanov et al., 2014; Vanderboor et al., 2020), we applied the ROCK inhibitors Y-27632 or fasudil to affirm this assumption. Both blockers prevented bleb formation (data not shown). Thus, we propose that, besides G_q

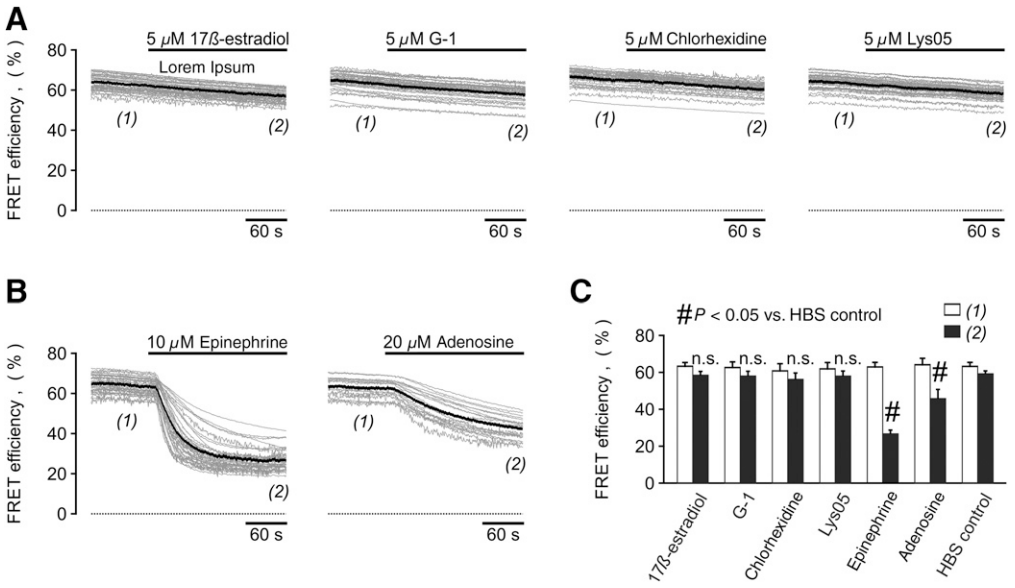

Fig. 7. FRET-based measurement of cAMP formation during the application of GPR30 agonists using an EPAC-derived biosensor. A possible impact of GPR30 agonists on intracellular cyclic adenosine monophosphate formation was evaluated by transiently transfecting $HEK293_{hGPR30\text{-}YFP}$ cells with a cDNA encoding an established EPAC-based FRET biosensor. (A) After 24 hours, FRET efficiencies in 34–36 single cells (gray lines) and their averaged values (black lines) were recorded before and during the application of 17β-estradiol, G-1, chlorhexidine, or Lys05 as indicated by the horizontal bars. Note the slight linear decline, which is caused by photobleaching the FRET acceptor YFP. (B) To validate cAMP measurements, positive controls with epinephrine and adenosine activating endogenously expressed β-adrenergic and adenosine receptors, respectively, were carried out. (C) Means and S.D. obtained from four to six independent biologic experiments performed as in (A and B). #$P < 0.05$, differences to buffer (HBS)-treated controls at time point *(2)*. n.s., no statistically significant differences to buffer controls.

coupling, hGPR30 may also activate heterotrimeric G proteins of the $G_{12/13}$ family, which is a frequently observed dual-coupling pattern for G_q-linked GPCRs.

Transiently Transfected GPR30 Pattern and Calcium Signals Differ in Various Cell Types. In the past, the results of GPR30 localization assays revealed conflicting patterns with reports on a predominant localization in the endoplasmic reticulum or in the plasma membrane (Revankar et al., 2005; Bologa et al., 2006; Funakoshi et al., 2006; Filardo et al., 2007; Otto et al., 2008). Since variations in the cellular localization patterns may depend on the cell types they are investigated in, we transiently transfected the expression plasmid encoding YFP-tagged hGPR30 into HeLa, COS-7, and MCF-7 cells, which endogenously express GPR30. Surprisingly, the plasma membrane localization of transiently expressed hGPR30-YFP in HEK293 cells was less prominent than in our stable $HEK293_{hGPR30\text{-}YFP}$ cell line and only observable in cells that express only small amounts of the fusion protein (Fig. 11A). When compared with the other cell lines, HEK293 cells followed by MCF-7 were visually the cell type with the highest abundance of hGPR30-YFP in the plasma membrane. In COS-7 and in HeLa cells, hGPR30-YFP seemed to be retained in the endoplasmic reticulum, as indicated by the reticular pattern and nuclear membrane residence of intracellularly retained hGPR30-YFP proteins (Fig. 11, D and G).

To examine whether the cellular distribution affects the efficacy of chlorhexidine or Lys05 to elicit functional Ca^{2+} mobilization signals, we performed single-cell $[Ca^{2+}]_i$ imaging experiments in all investigated cell types. After transient transfection of GPR30, chlorhexidine and Lys05 elicited a rise in basal $[Ca^{2+}]_i$ in all cell lines. In HEK293 and MCF-7 cells, 62%–67% of the transfected cells (as detected by their yellow fluorescence) responded to the addition of chlorhexidine or Lys05 with increases in $[Ca^{2+}]_i$ by more than 100 nM over their basal $[Ca^{2+}]_i$. In HeLa cells, rises in $[Ca^{2+}]_i$ occurred in 40%–64% of transfected cells but often with a delayed response when compared with HEK293 or MCF-7 cells (Fig. 11, H and I). A functional GPR30 activation in COS-7 cells by chlorhexidine or Lys05 could only provoked in 16%–25% of GPR30-expressing cells (Fig. 11, E and F). This observation was in line with the observed higher efficiency in plasma membrane targeting of the protein in HEK293 or MCF-7 cells compared with COS-7 and HeLa cells. Parental HEK293 (Fig. 2) or parental COS-7 and HeLa cells (data not shown) did not respond to the two GPR30 agonists. Parental MCF-7 cells showed transient and inhomogeneous $[Ca^{2+}]_i$ signals to the addition of 5 μM chlorhexidine that were also obtained when applying 0.05% DMSO as solvent control (Supplemental Fig. 7). Notably, agonist-induced $[Ca^{2+}]_i$ signals in transiently hGPR30-YFP–overexpressing MCF-7 signals were more uniform and stronger than in the untransfected or mock-transfected parental cell line. Taken together, we conclude that the newly identified GPR30 agonists, albeit eliciting more variable results in transiently transfected cells, were effective specific for GPR30 regardless of which cell line we used. Furthermore, diverse findings in past could rely on the use of various cell types in different laboratories.

Discussion

In this study, we identified three novel GPR30 agonists by performing an unbiased multiplexed screen of 31 GPRCs, including numerous orphan members. Our screening assay was based on measurement of intracellular Ca^{2+} concentrations with coexpressed G-protein α subunits 15/16 to enforce a convergence of GPCR signaling toward PLC activation with subsequent Ca^{2+} signals. Until now, GPR30 has been described as a receptor that induces cAMP production via a G_s

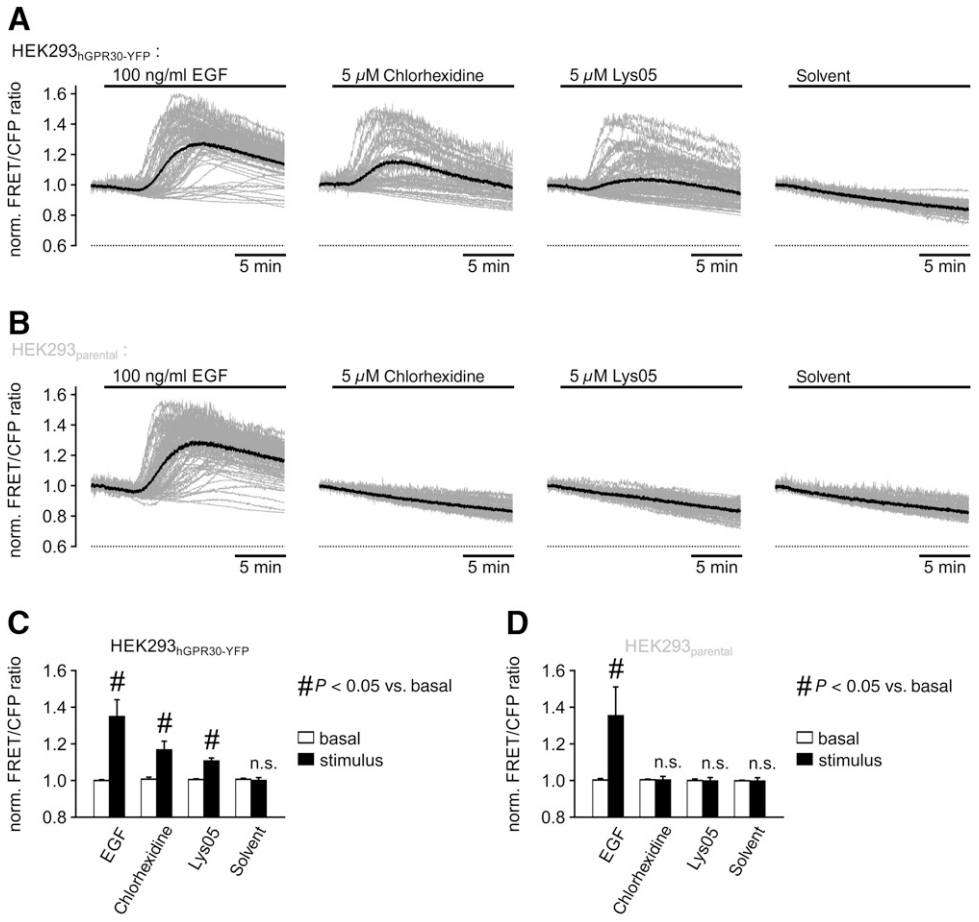

Fig. 8. Imaging of GPR30-induced ERK activity by using a FRET-based biosensor. $HEK293_{hGPR30\text{-}YFP}$ cells (A) or parental HEK293 (B) cells were transiently transfected with cDNA plasmids encoding a cytosolic ERK activity reporter 4 (cytoEKAR4) to investigate the effect of chlorhexidine and Lys05 on ERK activity. Shown are exemplary measurements of FRET signals obtained from 46–77 single cells (gray lines) and their averaged values (black lines), respectively. As positive controls, experiments with recombinant human epidermal growth factor (EGF) (100 ng/ml), activating endogenously expressed EGF receptors, were performed. The slight linear decline is caused by photobleaching of the FRET acceptor YFP during the experiment. (C and D) For statistical analysis, averaged values were obtained from five to six independent biologic experiments, performed as shown in (A and B) and corrected for photobleaching, and FRET signals before (white bars) and 10 minutes after agonist addition (black bars) were compared. Increases in FRET signals after the addition of chlorhexidine or Lys05 were recorded in $HEK293_{hGPR30\text{-}YFP}$ cells (C; $\#P < 0.05$, one-way ANOVA Dunn-Šidák), whereas parental HEK293 cells (D) showed no statistically significant ERK activation (n.s.).

pathway (Kanda and Watanabe, 2003; Thomas et al., 2005; Mo et al., 2013). Astonishingly, it has also been described to induce a Ca^{2+} mobilization in a PLC-independent manner (Revankar et al., 2005; Bologa et al., 2006; Ariazi et al., 2010) in both native and in GPR30-overexpressing cells. In addition, GPR30 mediates ERK-1/2 phosphorylation as well as phosphoinositide 3-kinase (PI3K) activation via transactivating epidermal growth factor receptors in breast cancer cell lines or in GPR30-overexpressing COS-7 cells (Filardo et al., 2000; Revankar et al., 2005). Of note, reported GPR30 agonists (Rosano et al., 2016), which are included in our Selleckchem library, failed to elicit increases in $[Ca^{2+}]_i$ despite favoring promiscuous coupling via $G\alpha_{15/16}$. By contrast, three compounds that have previously not been reported as GPCR agonists, namely chlorhexidine, Lys05, and 9-aminoacridine, emerged as agonists, with secondary screening results showing that GPR30 was the common target GPCR for all three compounds. Although the newly identified agonists may share structural motifs with an as yet unidentified physiologic GPR30 agonist, the assumption of a unified pharmacophore must not hold true. Notably, the AT_1 receptor as closest relative of GPR30 is a peptide receptor.

Our experiments provided several lines of evidence that signaling downstream of GPR30 was relayed via a canonical G_q-linked, PLC-dependent pathway, leading to Ca^{2+} mobilization, recruitment of diacylglycerol-sensitive PKC isoforms, and activation of the ERK pathway. Since previous studies did not show such canonical signaling properties, the different observations may deserve a closer analysis. In our hands, inhibitors of G_q, PLC, and $InsP_3$ receptors reliably and completely blocked Ca^{2+} signals regardless of which agonist we used. Depletion of $InsP_3$-sensitive Ca^{2+} stores by pretreating GPR30-expressing cells with thapsigargin abolished chlorhexidine-, Lys05-, and 9-aminoacridine–induced Ca^{2+} responses. Other groups negated efficacy of PLC inhibitor U73122 (Revankar et al., 2005) or got variable results when applying IP_3 receptor inhibitors 2-APB or xestopongin C in different cell types (Ariazi et al., 2010). Performing complementary CFP-PLC-δ_1 (PH) and PKCε-CFP translocation assays that indicate PIP_2 hydrolysis and generation of diacylglycerols, respectively, our study demonstrates robust coupling of GPR30 to PLC.

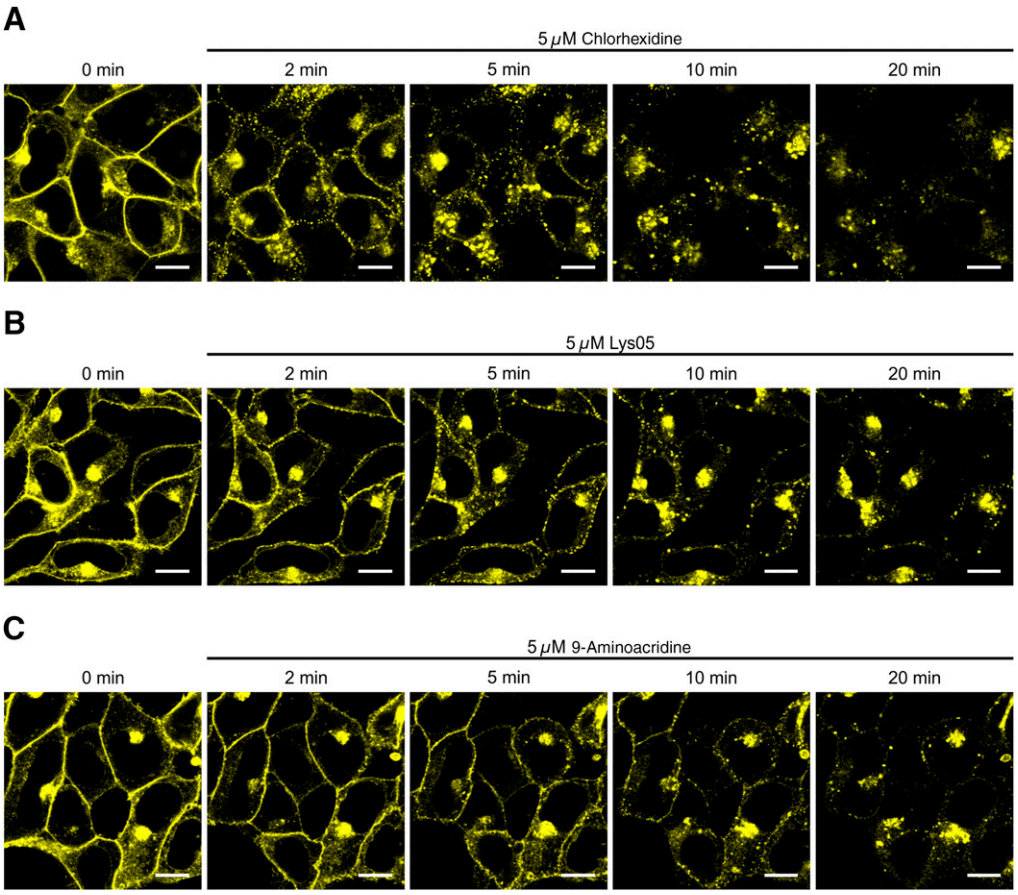

Fig. 9. Rapid and efficient internalization of hGPR30 in the continuous presence of newly identified agonists. Image series of hGPR30-YFP were taken by confocal laser-scanning microscopy in living $HEK293_{hGPR30\text{-}YFP}$ cells immediately before (0 min) and at the indicated times after stimulating cells with either 5 μM chlorhexidine (A), Lys05 (B), or 9-aminoacridine (C). Scale bars, 10 μM. Note that receptor clustering at or close to the plasma membrane precedes the internalization.

A canonical, PLC-driven Ca^{2+} mobilization response typically consists of a transient increase in $[Ca^{2+}]_I$, lasting for about 1 to 2 minute and terminating in slightly elevated levels. In GPR30-expressing HEK293 cells, we observed such a uniform time course in all imaged cells upon stimulation with the newly identified agonists. In previous studies using 17β-estradiol, 4-hydroxytamoxifen, or G-1, single-cell $[Ca^{2+}]_i$ imaging experiments showed atypical kinetic properties (Revankar et al., 2005; Bologa et al., 2006) or variable kinetic properties depending on the agonists and cell types used (Ariazi et al., 2010). When added at concentrations >10 μM, tamoxifen induced delayed and long-lasting Ca^{2+} signals in GPR30-overexpressing as well as in parental HEK293 cells, confirming earlier reports that found that tamoxifen and its metabolite

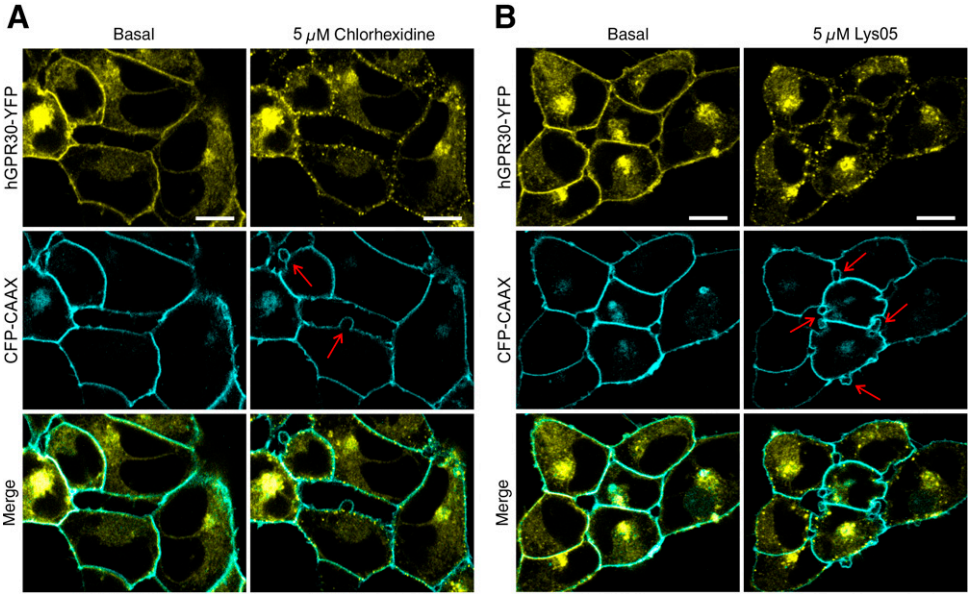

Fig. 10. Plasma membrane blebbing responses after hGPR30 stimulation with chlorhexidine and Lys05. Confocal laser-scanning images like shown in Fig. 8 but with $HEK293_{hGPR30\text{-}YFP}$ cells that were additionally stably cotransfected with a cDNA plasmid encoding a CAAX-box–modified and thereby plasma membrane-targeted cyan fluorescent protein (CFP-CAAX). Shortly after GPR30 activation with 5 μM chlorhexidine (A) or Lys05 (B), and during receptor clustering (upper panels), the CFP-delineated plasma membrane showed dynamic blebbing events (middle panels). Lower panels: overlay of YFP and CFP signals. Scale bars, 10 μM.

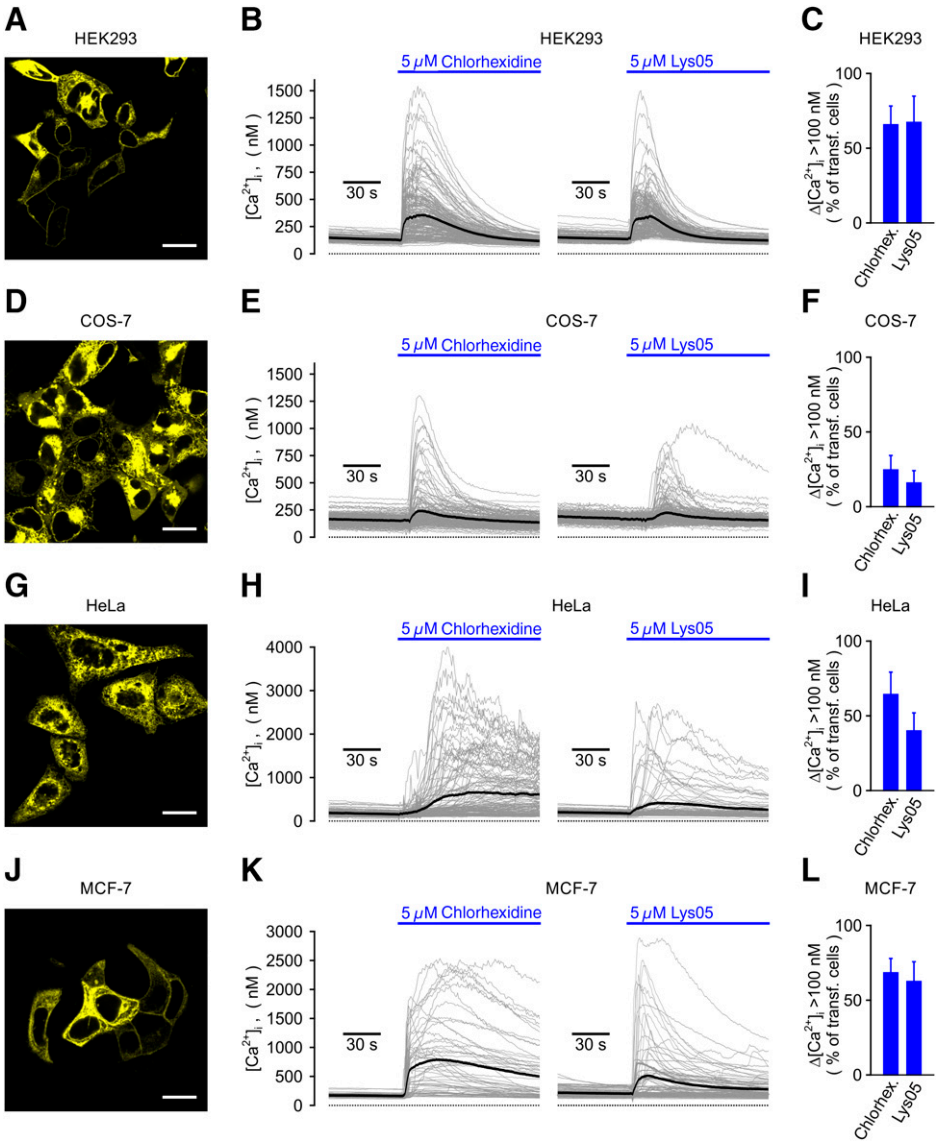

Fig. 11. Subcellular localization and $[Ca^{2+}]_i$ responses of transiently overexpressed hGPR30 in various cell lines. The cellular localization of human GPR30 and functional responsiveness to chlorhexidine and Lys05 were examined in HEK293 (A–C), COS-7 (D–F), HeLa (G–I), and MCF-7 cells (J–L). (A, D, G, and J) Representative confocal microscopy images of hGPR30-YFP in different cell lines 24 hours after transient transfection. Scale bar, 20 μM. (B, E, H, and K) Fluorometric single-cell $[Ca^{2+}]_i$ analysis in hGPR30-YFP–expressing HEK293, COS-7, HeLa, or MCF-7 cells was performed as described in Fig. 2C. Shown are exemplary measurements during chlorhexidine (left panels) or Lys05 (right panels) application. (C, F, I, and L) Means and S.D. of the percentage of transfected cells that responded during the application of the indicated hGPR30 agonists with increases in intracellular Ca^{2+} concentration by more than 100 nM. Data represent four to six independent measurements performed as in (B, E, H, and K).

interfere with cytosolic Ca^{2+} homeostasis in an estrogen receptor or GPR30-independent fashion (Zhang et al., 2000; Bollig et al., 2007; Asp et al., 2013). Our finding that 17β-estradiol and G-1 did not elicit Ca^{2+} responses in $HEK293_{hGPR30\text{-}YFP}$ cells is in line with observations in heterologously GPR30-expressing CHO-K1 cells (Otto et al., 2008). In MCF-7 cells, the reported GPR30 agonist G-1 induces Ca^{2+} efflux from the ER that is associated with ER stress and cell death (Vo et al., 2019). When applied at concentrations that activate GPR30, chlorhexidine and Lys05 elicited an increase in metabolic activity reminiscent of the comitogenic activity of numerous G_q -coupled receptors, including the GPR30-related AT_1 angiotensin-II receptor (Forrester et al., 2018). Although the initial characterization of G-1 included data that demonstrate a competition for binding of an estradiol derivative to GPR30, other studies failed to reproduce 17β-estradiol binding to GPR30 (Otto et al., 2008). Similar results were obtained by Pedram et al. (2006). Thus, the specific binding of estrogens to GPR30 is not undisputed.

Since initial evidence has suggested that activation of GPR30 triggers increases in cAMP concentrations, we wondered whether our GPR30 agonist may exert such a biased agonism toward PLC while maintaining some coupling to the G_s-cAMP pathway. To test this hypothesis, we used the EPAC-based sensitive cAMP-reporting biosensor. In $HEK293_{hGPR30\text{-}YFP}$ cells, this sensor was capable of detecting cAMP formation triggered by the endogenously expressed adenosine receptor or the β_2 adrenoceptor. In the same cells, neither recently reported (17β-estradiol, G-1) nor our newly identified GPR30 agonists chlorhexidine and Lys05 evoked detectable changes in cAMP levels. This observation

corroborates findings that COS-7 or HEK293 cells heterologously expressing GPR30 lacked enhanced cAMP formation after treatment with 17β-estradiol or G-1 (Otto et al., 2008; Broselid et al., 2014). Moreover, the latter authors observed a GPR30-mediated, but again 17β-estradiol- or G-1–independent, constitutive inhibition of cAMP formation and increased cAMP levels after siRNA knockdown of native GPR30 in MDCK cells. Recently, it has become clear that some GPCR agonists may shift the signaling toward specific G-protein families or arrestins. This phenomenon is commonly referred to as "biased agonism" (Bock and Bermudez, 2021). Although we cannot exclude that the newly identified GPR30 agonists may exert a biased agonism, the coupling of three chemically distinct agonists toward a canonical G_q pathway argues against such signaling bias.

There are also inconsistent data regarding the subcellular localization of GPR30. Several studies demonstrated that GPR30 is localized to the ER (Revankar et al., 2005; Bologa et al., 2006; Otto et al., 2008; Lin et al., 2009) or in the Golgi complex (Sakamoto et al., 2007). Other groups found GPR30 integrated into the plasma membrane (Thomas et al., 2005; Funakoshi et al., 2006; Filardo et al., 2007; Mo et al., 2013). Upon expression in different cell lines, we observed a YFP-tagged GPR30 mainly in the ER and in the plasma membrane, but the balance was strongly dependent on the cell type used. A pronounced plasma membrane localization was observable in HEK293 and MCF-7 cells, especially in cells that expressed low amounts of the protein. In COS-7 and HeLa cells, GPR30-YFP mostly accumulated in perinuclear endomembrane compartments. Such cell type– and expression density–dependent effects may explain the diverging observations, especially when using transiently transfected cells.

The identification of reliably acting GPR30 agonists that initiate a canonical G_q- and PLC-linked signaling pathway may pave the way toward an investigation of real physiologic functions of this GPCR and overcoming the state of contradictory results in the field. A genetic knockin mouse model, which harbors a lacZ reporter in the GPR30 locus, has revealed a major expression in vascular endothelial cells of multiple tissues and also in smooth muscle cells and in pericytes of brain vessels (Isensee et al., 2009). Female GPR30 knockout mice showed a blood pressure elevation at the age of 9 months (Mårtensson et al., 2009). In conjunction with the flow-induced upregulation of GPR30 expression in human umbilical vein endothelial cells (HUVEC) (Takada et al., 1997), this finding implies that GPR30 may play a role in regulating endothelial functions. Furthermore, the ubiquitous expression profile and the similarity to the G_q- and $G_{12/13}$-coupling AT_1 receptor (Feng and Gregor, 1997) would fit to a model that GPR30 is expressed in blood vessels. Recently, Tutzauer et al. (2021) attempted to confirm a vasodilatory function of GPR30 by measuring the relaxation of caudal arteries from wild-type as well as from GPR30 knockout mice while treating them with the previously proposed GPR30-specific agonists G-1 and 17β-estradiol. They found that arteries from GPR30-deficient mice relaxed with the same potency and efficacy as in wild-type mice. In addition, various cellular expression models showed no effects of G-1 or 17β-estradiol and prompted them to state that "classifying GPR30 as an estrogen receptor and G-1 as a specific GPR30 agonist is unfounded." Based on our data, we agree with their conclusion and hope that the discovery of a reliably acting GPR30 agonist and the finding of its coupling to the canonical G_q-phospholipase C signaling pathway may be instrumental in more unambiguously identifying the physiologic functions of GPR30.

Authorship Contributions

Participated in research design: Urban, Schaefer.

Conducted experiments: Urban, Leonhardt.

Performed data analysis: Urban, Schaefer.

Wrote or contributed to the writing of the manuscript: Urban, Schaefer.

References

Ariazi EA, Brailoiu E, Yerrum S, Shupp HA, Slifker MJ, Cunliffe HE, Black MA, Donato AL, Arterburn JB, Oprea TI, et al. (2010) The G protein-coupled receptor GPR30 inhibits proliferation of estrogen receptor-positive breast cancer cells. *Cancer Res* **70**:1184–1194.

Aronica SM, Kraus WL, and Katzenellenbogen BS (1994) Estrogen action via the cAMP signaling pathway: stimulation of adenylate cyclase and cAMP-regulated gene transcription. *Proc Natl Acad Sci USA* **91**:8517–8521.

Asp ML, Martindale JJ, and Metzger JM (2013) Direct, differential effects of tamoxifen, 4-hydroxytamoxifen, and raloxifene on cardiac myocyte contractility and calcium handling. *PLoS One* **8**:e78768.

Bock A and Bermudez M (2021) Allosteric coupling and biased agonism in G protein-coupled receptors. *FEBS J* **288**:2513–2528.

Bollig A, Xu L, Thakur A, Wu J, Kuo TH, and Liao JD (2007) Regulation of intracellular calcium release and PP1alpha in a mechanism for 4-hydroxytamoxifen-induced cytotoxicity. *Mol Cell Biochem* **305**:45–54.

Bologa CG, Revankar CM, Young SM, Edwards BS, Arterburn JB, Kiselyov AS, Parker MA, Tkachenko SE, Savchuck NP, Sklar LA, et al. (2006) Virtual and biomolecular screening converge on a selective agonist for GPR30. *Nat Chem Biol* **2**:207–212.

Broselid S, Berg KA, Chavera TA, Kahn R, Clarke WP, Olde B, and Leeb-Lundberg LMF (2014) G protein-coupled receptor 30 (GPR30) forms a plasma membrane complex with membrane-associated guanylate kinases (MAGUKs) and protein kinase A-anchoring protein 5 (AKAP5) that constitutively inhibits cAMP production. *J Biol Chem* **289**:22117–22127.

Carmeci C, Thompson DA, Ring HZ, Francke U, and Weigel RJ (1997) Identification of a gene (GPR30) with homology to the G-protein-coupled receptor superfamily associated with estrogen receptor expression in breast cancer. *Genomics* **45**:607–617.

Charras GT (2008) A short history of blebbing. *J Microsc* **231**:466–478.

Edelstein A, Amodaj N, Hoover K, Vale R, and Stuurman N (2010) Computer control of microscopes using μManager. *Curr Protoc Mol Biol* **Chapter 14**:Unit14.20.

Feng Y and Gregor P (1997) Cloning of a novel member of the G protein-coupled receptor family related to peptide receptors. *Biochem Biophys Res Commun* **231**:651–654.

Filardo E, Quinn J, Pang Y, Graeber C, Shaw S, Dong J, and Thomas P (2007) Activation of the novel estrogen receptor G protein-coupled receptor 30 (GPR30) at the plasma membrane. *Endocrinology* **148**:3236–3245.

Filardo EJ, Quinn JA, Bland KI, and Frackelton Jr AR (2000) Estrogen-induced activation of Erk-1 and Erk-2 requires the G protein-coupled receptor homolog, GPR30, and occurs via trans-activation of the epidermal growth factor receptor through release of HB-EGF. *Mol Endocrinol* **14**:1649–1660.

Filardo EJ, Quinn JA, Frackelton Jr AR, and Bland KI (2002) Estrogen action via the G protein-coupled receptor, GPR30: stimulation of adenylyl cyclase and cAMP-mediated attenuation of the epidermal growth factor receptor-to-MAPK signaling axis. *Mol Endocrinol* **16**:70–84.

Forrester SJ, Booz GW, Sigmund CD, Coffman TM, Kawai T, Rizzo V, Scalia R, and Eguchi S (2018) Angiotensin II signal transduction: an update on mechanisms of physiology and pathophysiology. *Physiol Rev* **98**:1627–1738.

Funakoshi T, Yanai A, Shinoda K, Kawano MM, and Mizukami Y (2006) G protein-coupled receptor 30 is an estrogen receptor in the plasma membrane. *Biochem Biophys Res Commun* **346**:904–910.

Häfner S, Urban N, and Schaefer M (2019) Discovery and characterization of a positive allosteric modulator of transient receptor potential canonical 6 (TRPC6) channels. *Cell Calcium* **78**:26–34.

Hauser AS, Gloriam DE, Bräuner-Osborne H, and Foster SR (2020) Novel approaches leading towards peptide GPCR de-orphanisation. *Br J Pharmacol* **177**:961–968.

Hellwig N, Plant TD, Janson W, Schäfer M, Schultz G, and Schaefer M (2004) TRPV1 acts as proton channel to induce acidification in nociceptive neurons. *J Biol Chem* **279**:34553–34561.

Isensee J, Meoli L, Zazzu V, Nabzdyk C, Witt H, Soewarto D, Effertz K, Fuchs H, Gailus-Durner V, Busch D, et al. (2009) Expression pattern of G protein-coupled receptor 30 in LacZ reporter mice. *Endocrinology* **150**:1722–1730.

Kanda N and Watanabe S (2003) 17Beta-estradiol enhances the production of nerve growth factor in THP-1-derived macrophages or peripheral blood monocyte-derived macrophages. *J Invest Dermatol* **121**:771–780.

Keyes J, Ganesan A, Molinar-Inglis O, Hamidzadeh A, Zhang J, Ling M, Trejo J, Levchenko A, and Zhang J (2020) Signaling diversity enabled by Rap1-regulated plasma membrane ERK with distinct temporal dynamics. *eLife* **9**:e57410.

Klarenbeek J, Goedhart J, van Batenburg A, Groenewald D, and Jalink K (2015) Fourth-generation epac-based FRET sensors for cAMP feature exceptional brightness, photostability and dynamic range: characterization of dedicated sensors for FLIM, for ratiometry and with high affinity. *PLoS One* **10**:e0122513.

Kostenis E, Waelbroeck M, and Milligan G (2005) Techniques: promiscuous Galpha proteins in basic research and drug discovery. *Trends Pharmacol Sci* **26**:595–602.

Laschet C, Dupuis N, and Hanson J (2018) The G protein-coupled receptors deorphanization landscape. *Biochem Pharmacol* **153**:62–74.

Lenz JC, Reusch HP, Albrecht N, Schultz G, and Schaefer M (2002) Ca^{2+}-controlled competitive diacylglycerol binding of protein kinase C isoenzymes in living cells. *J Cell Biol* **159**:291–302.

Lin BC, Suzawa M, Blind RD, Tobias SC, Bulun SE, Scanlan TS, and Ingraham HA (2009) Stimulating the GPR30 estrogen receptor with a novel tamoxifen analogue activates SF-1 and promotes endometrial cell proliferation. *Cancer Res* **69**:5415–5423.

Liu J, Conklin BR, Blin N, Yun J, and Wess J (1995) Identification of a receptor/G-protein contact site critical for signaling specificity and G-protein activation. *Proc Natl Acad Sci USA* **92**:11642–11646.

Mårtensson UEA, Salehi SA, Windahl S, Gomez MF, Swärd K, Daszkiewicz-Nilsson J, Wendt A, Andersson N, Hellstrand P, Grände P-O, et al. (2009) Deletion of the G protein-coupled receptor 30 impairs glucose tolerance, reduces bone growth, increases blood pressure, and eliminates estradiol-stimulated insulin release in female mice. *Endocrinology* **150**:687–698.

Mo Z, Liu M, Yang F, Luo H, Li Z, Tu G, and Yang G (2013) GPR30 as an initiator of tamoxifen resistance in hormone-dependent breast cancer. *Breast Cancer Res* **15**:R114.

Offermanns S and Simon MI (1995) G alpha 15 and G alpha 16 couple a wide variety of receptors to phospholipase C. *J Biol Chem* **270**:15175–15180.

Otto C, Rohde-Schulz B, Schwarz G, Fuchs I, Klewer M, Brittain D, Langer G, Bader B, Prelle K, Nubbemeyer R, et al. (2008) G protein-coupled receptor 30 localizes to the endoplasmic reticulum and is not activated by estradiol. *Endocrinology* **149**:4846–4856.

Pedram A, Razandi M, and Levin ER (2006) Nature of functional estrogen receptors at the plasma membrane. *Mol Endocrinol* **20**:1996–2009.

Pfeil EM, Brands J, Merten N, Vögtle T, Vescovo M, Rick U, Albrecht I-M, Heycke N, Kawakami K, Ono Y, et al. (2020) Heterotrimeric G Protein Subunit Gαq Is a Master Switch for Gβγ-Mediated Calcium Mobilization by Gi-Coupled GPCRs. *Mol Cell* **80**:940–954.e6.

Purvanov V, Holst M, Khan J, Baarlink C, and Grosse R (2014) G-protein-coupled receptor signaling and polarized actin dynamics drive cell-in-cell invasion. *eLife* **3**:e02786.

Revankar CM, Cimino DF, Sklar LA, Arterburn JB, and Prossnitz ER (2005) A transmembrane intracellular estrogen receptor mediates rapid cell signaling. *Science* **307**:1625–1630.

Ritscher L, Engemaier E, Stäubert C, Liebscher I, Schmidt P, Hermsdorf T, Römpler H, Schulz A, and Schöneberg T (2012) The ligand specificity of the G-protein-coupled receptor GPR34. *Biochem J* **443**:841–850.

Rosano C, Ponassi M, Santolla MF, Pisano A, Felli L, Vivacqua A, Maggiolini M, and Lappano R (2016) Macromolecular modelling and docking simulations for the discovery of selective GPER ligands. *AAPS J* **18**:41–46.

Sakamoto H, Matsuda K, Hosokawa K, Nishi M, Morris JF, Prossnitz ER, and Kawata M (2007) Expression of G protein-coupled receptor-30, a G protein-coupled membrane estrogen receptor, in oxytocin neurons of the rat paraventricular and supraoptic nuclei. *Endocrinology* **148**:5842–5850.

Schaefer M, Albrecht N, Hofmann T, Gudermann T, and Schultz G (2001) Diffusion-limited translocation mechanism of protein kinase C isotypes. *FASEB J* **15**:1634–1636.

Sinnecker D and Schaefer M (2004) Real-time analysis of phospholipase C activity during different patterns of receptor-induced Ca^{2+} responses in HEK293 cells. *Cell Calcium* **35**:29–38.

Sriram K and Insel PA (2018) G protein-coupled receptors as targets for approved drugs: how many targets and how many drugs? *Mol Pharmacol* **93**:251–258.

Sugo T, Tachimoto H, Chikatsu T, Murakami Y, Kikukawa Y, Sato S, Kikuchi K, Nagi T, Harada M, Ogi K, et al. (2006) Identification of a lysophosphatidylserine receptor on mast cells. *Biochem Biophys Res Commun* **341**:1078–1087.

Takada Y, Kato C, Kondo S, Korenaga R, and Ando J (1997) Cloning of cDNAs encoding G protein-coupled receptor expressed in human endothelial cells exposed to fluid shear stress. *Biochem Biophys Res Commun* **240**:737–741.

Thomas P, Pang Y, Filardo EJ, and Dong J (2005) Identity of an estrogen membrane receptor coupled to a G protein in human breast cancer cells. *Endocrinology* **146**:624–632.

Tutzauer J, Gonzalez de Valdivia E, Swärd K, Alexandrakis Eilard I, Broselid S, Kahn R, Olde B, and Leeb-Lundberg LMF (2021) Ligand-independent G protein-coupled estrogen receptor/G protein-coupled receptor 30 activity: lack of receptor-dependent effects of G-1 and 17β-estradiol. *Mol Pharmacol* **100**:271–282.

Vanderboor CMG, Thibeault PE, Nixon KCJ, Gros R, Kramer J, and Ramachandran R (2020) Proteinase-activated receptor 4 activation triggers cell membrane blebbing through RhoA and β-arrestin. *Mol Pharmacol* **97**:365–376.

Vo DH, Hartig R, Weinert S, Haybaeck J, and Nass N (2019) G-Protein-Coupled Estrogen Receptor (GPER)-Specific Agonist G1 Induces ER Stress Leading to Cell Death in MCF-7 Cells. *Biomolecules* **9**:503.

Zhang W, Couldwell WT, Song H, Takano T, Lin JH, and Nedergaard M (2000) Tamoxifen-induced enhancement of calcium signaling in glioma and MCF-7 breast cancer cells. *Cancer Res* **60**:5395–5400.

Address correspondence to: Dr. Michael Schaefer, Universität Leipzig, Härtelstr. 16-18, 4107 Leipzig, Germany. E-mail: michael.schaefer@medizin.uni-leipzig.de

Supplemental Figures to MOLPHARM-AR-2022-000580

Molecular Pharmacology

Multiplex GPCR screen reveals reliably acting agonists and a Gq-phospholipase C coupling mode of GPR30/GPER1

Nicole Urban, Marion Leonhardt, and Michael Schaefer

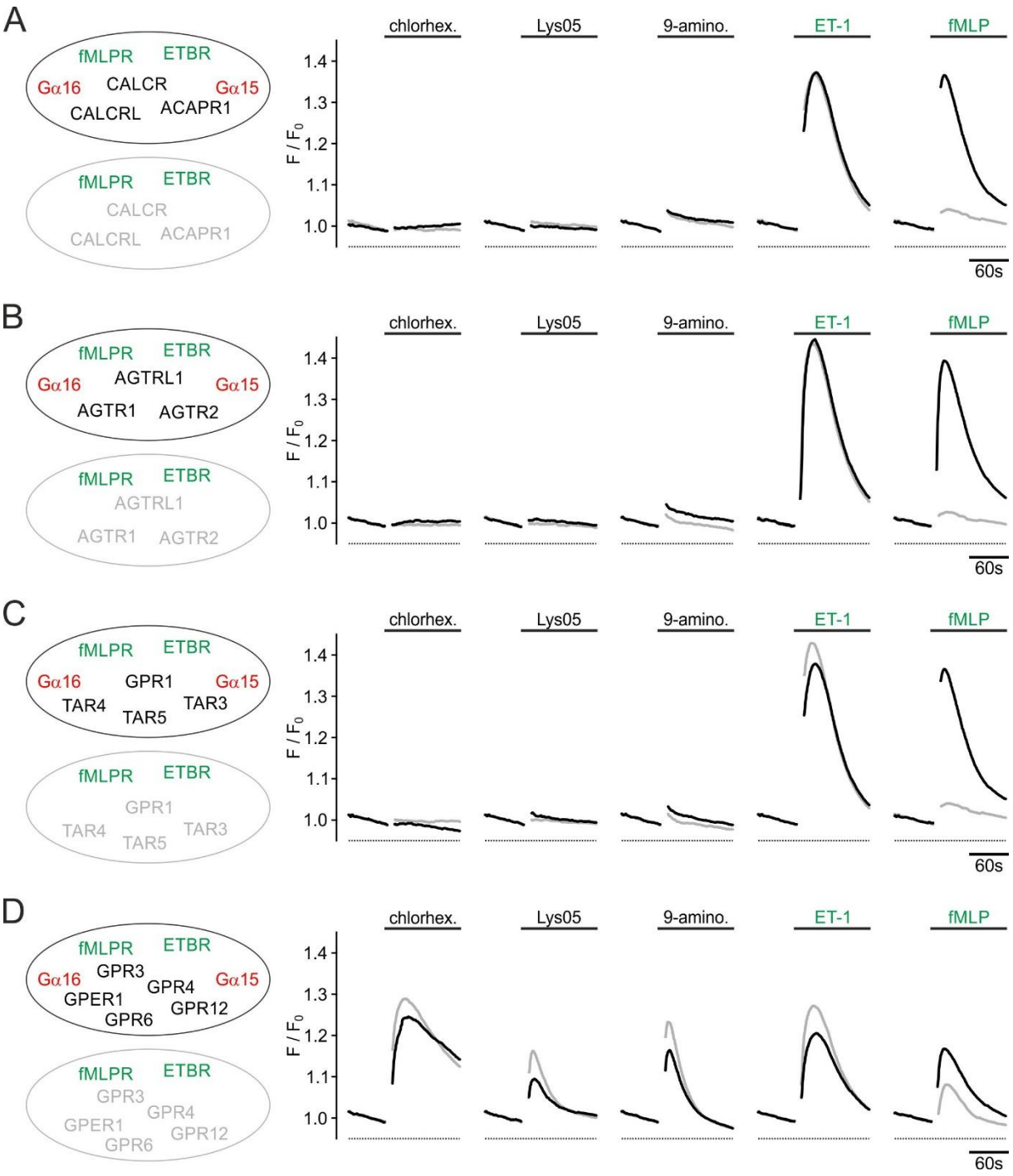

Suppl. Fig. 1: Identification of cDNA plasmid sub-pools that confer sensitivity to the primary hits.

The cDNA plasmids contained in transfection mixture 1 (see Fig. 1A) were divided into less complex sub-pools, containing 3-5 instead of 15 different plasmids (A-D). Plasmid sub-pools were generated with added FP_1 and ET_B receptors as controls, and with (upper circles; black lines) or without (lower circles; grey lines) adding $G\alpha_{15}$- and $G\alpha_{16}$-encoding plasmids, and transiently transfected in HEK293 cells. 24 h after transfection, HEK293 cells were harvested and loaded with fluo-4/AM, and monitored by multiwell FLIPR measurements (right panels) during the addition of chlorhexidine (20 µM), Lys05 (20 µM), 9-aminoacridine (20 µM), endothelin (10 nM) or fMLP (100 nM). Shown are resulting fluorescence signals obtained with (black lines) or without (grey lines) co-expressed $G\alpha_{15}$ and $G\alpha_{16}$. The transfection mix including GPR3, GPR4, GPR6, GPR12 and GPER1/GPR30 was the only one that induced an increase in fluo-4 fluorescence intensities after application of chlorhexidine, Lys05 or 9-aminoacridine (D).

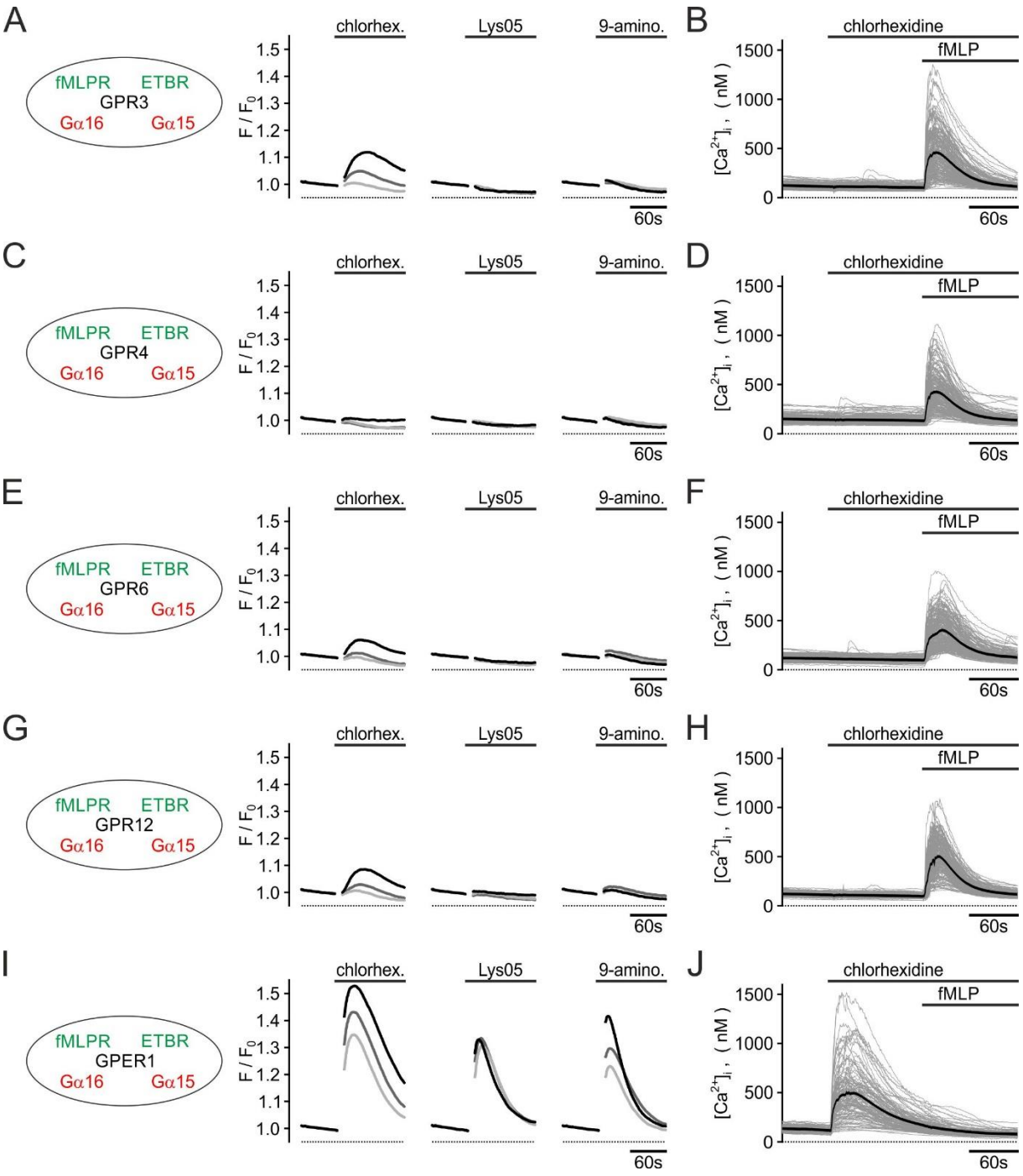

Suppl. Fig. 2: GPER1/GPR30 confers sensitivity to stimulation with chlorhexidine, Lys05 or 9-aminoacridine

(A, C, E, G, I) Combinations of cDNA plasmids that were generate to pinpoint the plasmid that confers responsiveness to the primary hits were assembled as illustrated in the left panels, and multiwell Ca^{2+} analyses (right panels) that were performed 24 hours after transient co-transfection of these cDNA plasmids, and fluo-4/AM-loading of cell suspensions. The activators chlorhexidine, Lys05 or 9-aminoacridine were injected to single wells and mixed to obtain final concentrations of 20 µM (black lines), 10 µM (middle grey lines) or 5 µM (light grey lines). Panel I reveals that GPER1/GPR30 was responsible for intracellular Ca^{2+} signals induced by all three compounds. (B, D, F, H, J) Since 10-20 µM chlorhexidine also induced small responses in GPR3-, GPR4-, GPR6- or GPR12-expressing HEK293 cells, we performed single cell $[Ca^{2+}]_i$ analyses with the same transfection compositions indicated in (A;C;E;G;I; left panels). Shown are time courses of $[Ca^{2+}]_i$ in 117 to 202 single cells (grey lines) along with the averaged signal (black line) during subsequent addition of 10 µM chlorhexidine and 100 nM fMLP as control. Note the response to chlorhexidine in GPER1/GPR30-expressing cells and the lack of a second response to 100 nM fMLP, indicating heterologous desensitization.

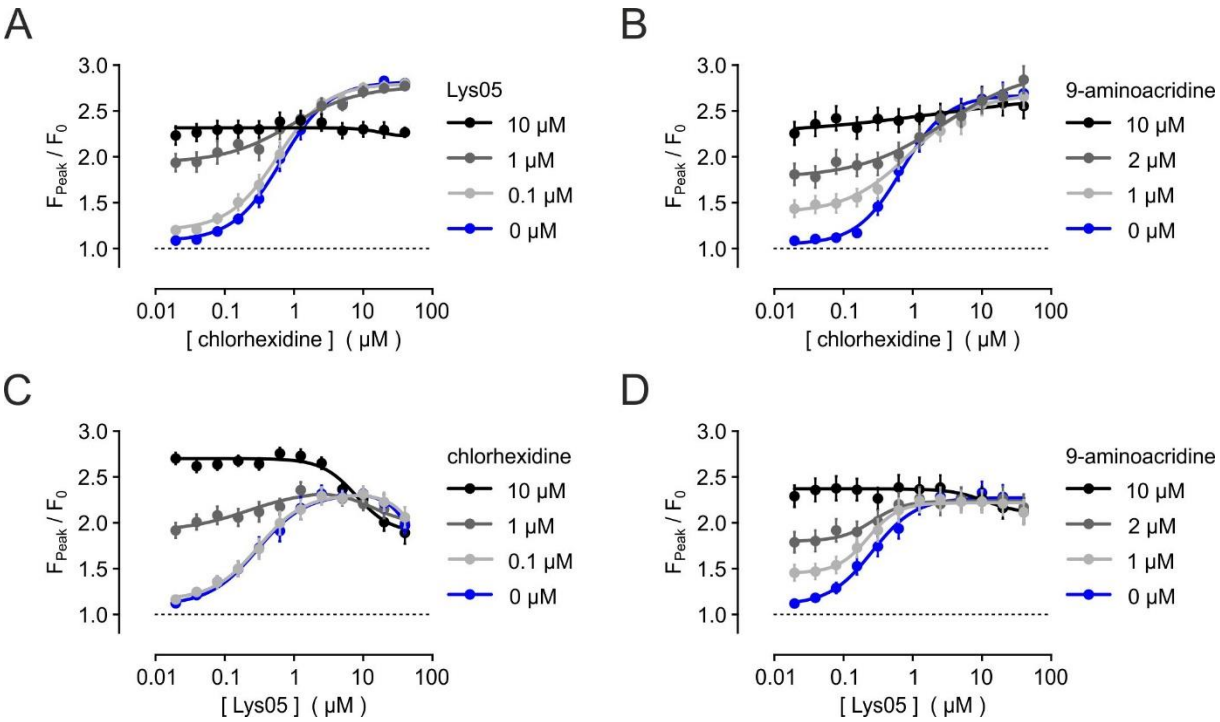

Suppl. Fig. 3: Measurement of allosteric relationship between new GPR30 agonists.

Fluo-4-loaded HEK293$_{hGPR30\text{-}YFP}$ cells were measured in a FLIPR device like described in Figure 2B, and acutely exposed to serially diluted chlorhexidine (A, B) or Lys05 (C, D) in combination with the indicated concentrations of a second GPR30 agonist. Shown are averaged fluorescence peak signals (F_{Peak}) and S.E. normalized to initial fluorescence (F_0) calculated from 3 independent experiments, performed in duplicates, each.

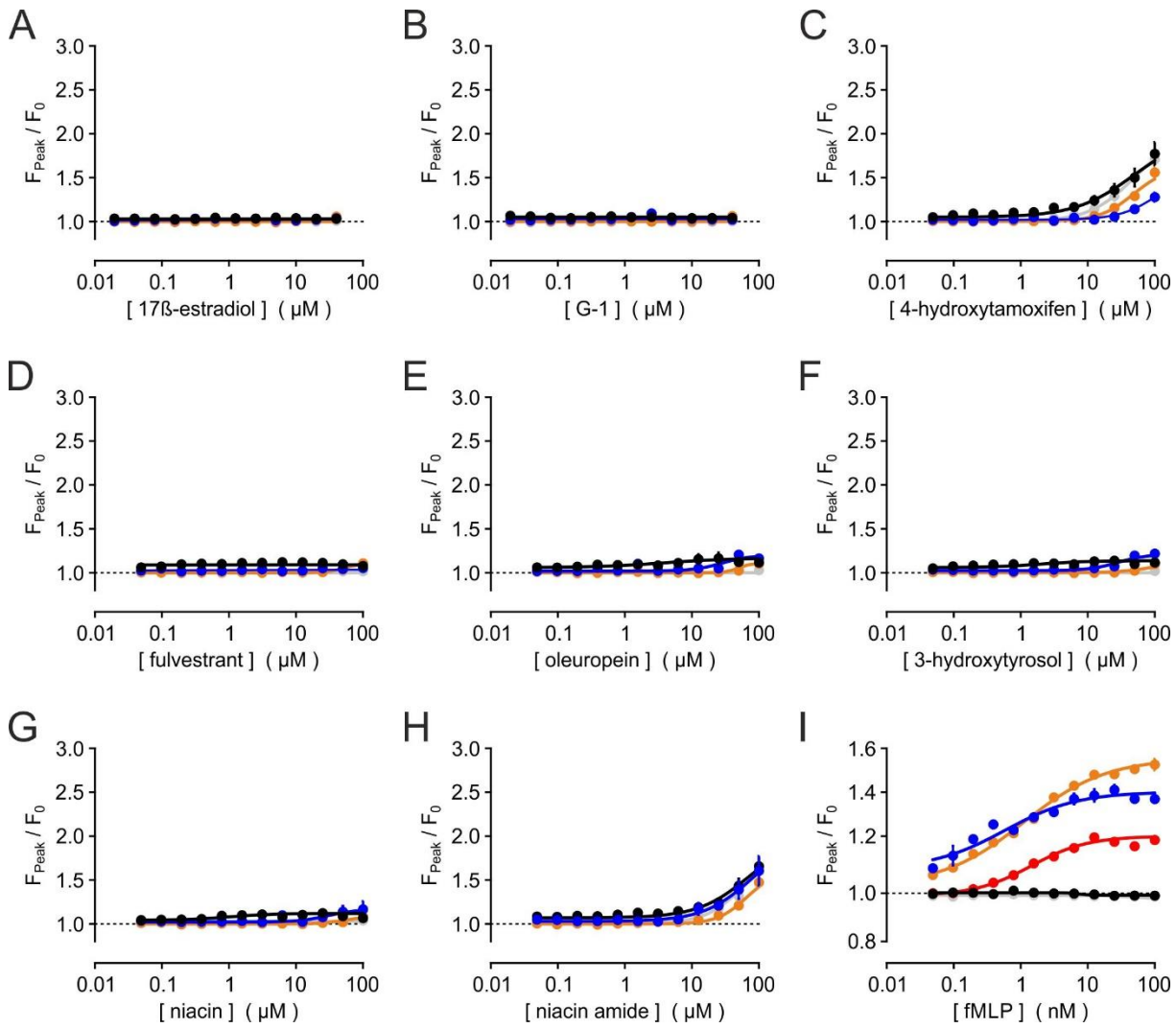

Suppl. Fig. 4: Concentration response curves of reported GPR30 agonists.

Parental HEK293 cells (grey symbols and lines), HEK293$_{hGPR30\text{-}YFP}$ cells (black symbols and lines), and HEK293$_{hGPR30\text{-}YFP}$ cells transiently transfected with FPR1 (blue and red symbols and lines) or with FPR1, Gα_{15} and Gα_{16} (orange symbols and lines) were loaded with the Ca^{2+} indicator fluo-4/AM, washed, and dispensed into 384-well plates. Fluorescence signals were imaged in a FLIPR-like device, and cells were exposed to the indicated, serially diluted reported GPR30 agonists for 5 min (A-H) or with serially diluted fMLP (I) with (blue symbols and lines) or without a prestimulation with 100 µM carbachol, applied 5 min prior to the fMLP addition. Shown are the aggregated fluorescence peak responses (F_{Peak}) normalized to the basal intensities (F_0) obtained in 3-6 independent transfection experiments, performed in duplicates, each. Note that reported GPER1/GPR30 agonists failed to induce $[Ca^{2+}]_i$ signals that exceed those seen in untransfected parental HEK293 cells.

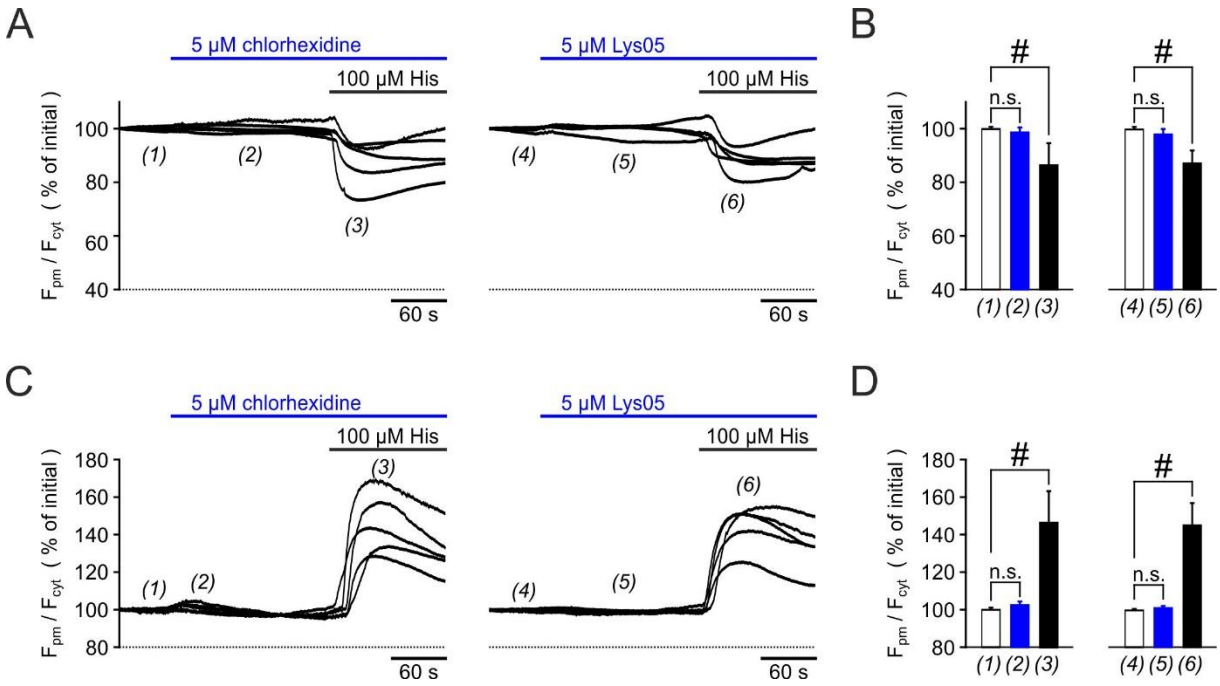

Suppl. Fig. 5: Translocation of CFP-PLC-δ_1(PH) and PKCε–CFP in parental HEK293 cells during chlorhexidine and Lys05 application.

Parental HEK293 cells were transiently transfected with cDNA plasmids encoding CFP-PLC-δ_1(PH) or PKCε-CFP as mentioned in Figure 6, but additionally with a histamine H_1 receptor as positive control. (A, C) Shown are the changes of PLC-δ_1(PH) or PKCε fluorescence signals in confocal time-lapse microscopy represented as plasma membrane (F_{pm}) to cytosol (F_{cyt}) ratio during addition of chlorhexidine or Lys05 and subsequent histamine. Black lines display averaged data from 3-9 cells measured in 5 independent experiments. (B, D) Statistical analysis (#: $p < 0.05$ in One-Way ANOVA Dunn-Sidak) of values at the indicated time points in (A, C). Application of hGPR30 agonists induced no significant change of CFP-PLC-δ_1(PH) or PKCε-CFP distribution in parental HEK293 cells, while the control agonist histamine (100 µM) induced robust translocation signals.

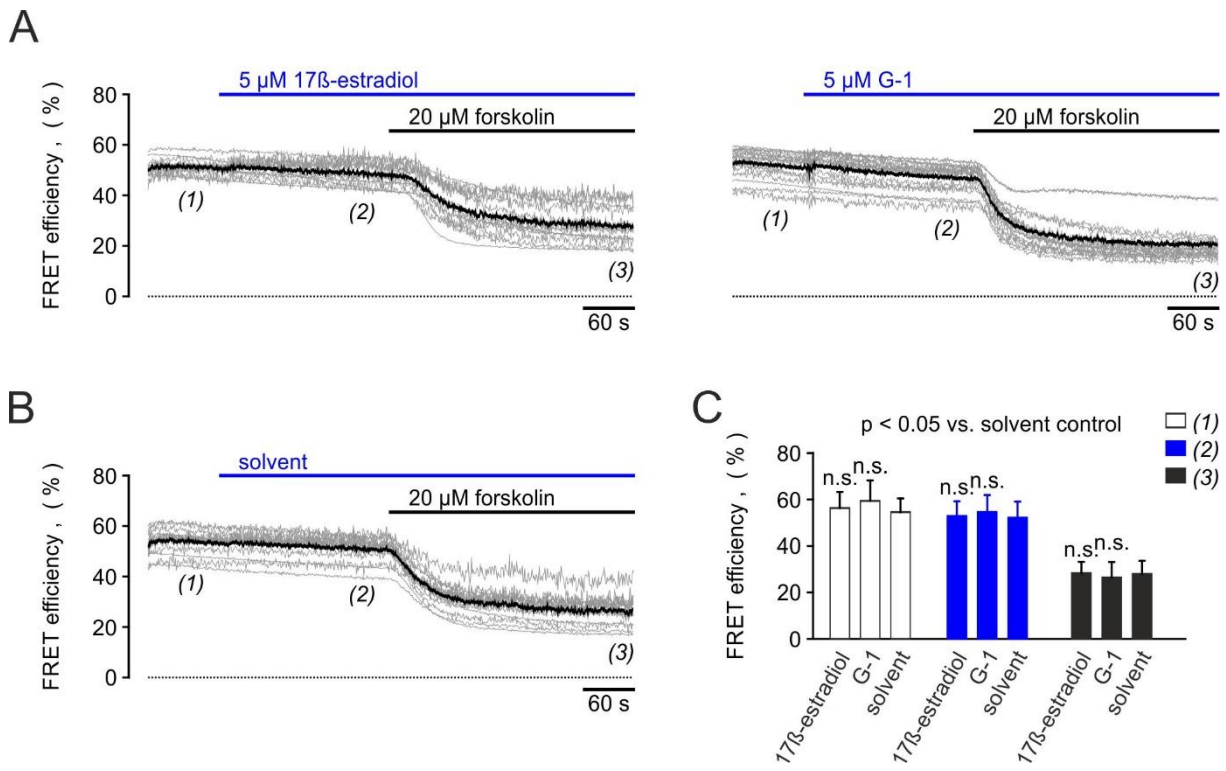

Suppl. Fig. 6: FRET-based measurement of cAMP formation in MCF-7 cells, applying the reported hGPR30 agonists 17ß-estradiol and G-1.

MCF-7 breast cancer cells that have been reported to endogenously express GPR30 were transiently transfected with cDNAs encoding the EPAC-based FRET biosensor as described in Figure 7 and additionally with hGPR30. After 24 hours, FRET efficiencies were measured during addition of published GPR30 agonists or DMSO to cells. In a second step, the adenylyl cyclase activator forskolin was applied in each experiment as positive controls. (A, B) Representative experiments for 17ß-estradiol, G-1 or solvent control show recordings in 14-18 single cells (grey lines) and their averaged values (black lines). (C) Means and S.D. at the indicated time points obtained from 6 independent experiments performed as in (A, B). There were no statistically significant (n.s.) differences between responses after addition of reported GPR30 agonists or the respective solvent controls (One-Way ANOVA Dunn-Sidak).

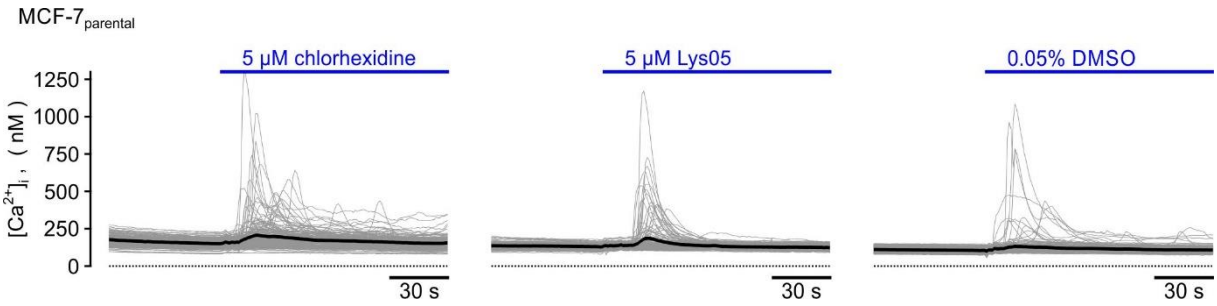

Suppl. Fig. 7: Ca^{2+} signals in parental MCF-7 cells.

MCF-7 cells were loaded with Fura-2, and subjected to microfluorometric single-cell $[Ca^{2+}]_i$ analysis. Few cells respond to GPR30 agonist or solvent (DMSO) addition. Note the stronger $[Ca^{2+}]_i$ responses in MCF-7 cells after transient expression of GPR30 shown in Fig. 10K of the main manuscript.